JOURNAL OF PETROLOGY

Journal of Petrology, 2016, Vol. 57, No. 11&12, 2081–2104
doi: 10.1093/petrology/egw073
Original Article

OXFORD

The Meaning of Global Ocean Ridge Basalt Major Element Compositions

Yaoling Niu[1,2,3]*

[1]Institute of Oceanology, Chinese Academy of Sciences, Qingdao, 266071, China; [2]Department of Earth Sciences, Durham University, Durham DH1 3LE, UK; [3]Laboratory for Marine Geology, Qingdao National Laboratory For Marine Science and Technology, Qingdao 266061, China

*Corresponding author. Department of Earth Sciences, Durham University, Durham DH1 3LE, UK. Telephone: +44-19-1334-2311. Fax: +44-19-1334-2301. E-mail: yaoling.niu@durham.ac.uk

Received April 12, 2016; Accepted December 16, 2016

ABSTRACT

Mid-ocean ridge basalts (MORB) are arguably the most abundant and also the simplest igneous rocks on the Earth. A correct understanding of their petrogenesis thus sets the cornerstone of igneous petrogenesis in general and also forms the foundation for studying mantle dynamics. Because major element compositions determine the mineralogy, phase equilibria and physical properties of rocks and magmas, understanding global MORB major element systematics is of prime importance. The correlated large MORB major element compositional variations are well understood as the result of cooling-dominated crustal-level processes (e.g. fractional crystallization, magma mixing, melt–rock assimilation or reaction, and other aspects of complex open-magma chamber processes), but it remains under debate what messages MORB major elements may carry about mantle sources and processes. To reveal mantle messages, it is logical to correct MORB melts for the effects of crustal-level processes to Mg# $\geq$ 0·72 to be in equilibrium with mantle olivine of $\geq Fo_{90}$. Such corrected MORB major element (e.g. Si_{72}, Ti_{72}, Al_{72}, Fe_{72}, Mg_{72}, Ca_{72} and Na_{72}) compositional variations thus reflect fertile mantle compositional variation, composition-controlled mantle physical property variation (e.g. density and solidus), variation in the extent and pressure of melting, and uncertainties associated with the correction. The correction-related uncertainties can be removed through justified heavy averaging. Because ridge axial depth variation ($\sim$0 to $\sim$6000 m below sea level) and plate spreading rate variation ($<$10 to $>$150 mm a^{-1}) are the two largest known physical variables along the global ocean ridge system, possible correlations of MORB major element compositions at Mg# $\geq$ 0·72 with these two physical variables are expected to reveal intrinsic controls on global MORB petrogenesis and ocean ridge dynamics. Indeed, global MORB major element data averaged with respect to both ridge axial depth intervals and ridge spreading rate intervals show significant first-order correlations. These correlations lead to the conclusion that the ridge axial depth variation and MORB chemistry variation are two different effects of a common cause, induced by fertile mantle compositional variation. The latter determines (1) variation in both composition and mode of mantle mineralogy, (2) variation of mantle density, (3) variation of ridge axial depth, (4) source-inherited MORB compositional variation, (5) density-controlled variation in the maximum extent of mantle upwelling, (6) apparent variation in the extent of melting, and (7) the correlated variation of MORB chemistry with ridge axial depth. These correlations also confirm the recognition that the extent of mantle melting increases with, and is caused by, increasing plate spreading rate. Mantle temperature variation could play a part, but its overstated role in the literature results from a basic error (1) in treating ridge axial depth variation as solely caused by mantle temperature variation by ignoring the intrinsic control of mantle composition, (2) in treating mantle plume-influenced ridges (e.g. Iceland) as normal ridges of plate spreading origin, and (3) in treating seismic low velocity at great depths ($>$300 km) beneath these mantle plume-influenced ridges as evidence for hot ridge mantle. There is no evidence for large mantle temperature variation beneath ridges away from mantle plumes. The suggested conclusions of this study may continue to be

debated, but they are most objective, and are most consistent with petrological, geochemical, geological and geophysical principles and observations.

Key words: mid-ocean ridges; MORB chemistry variation; MORB petrogenesis; mantle melting; fertile mantle compositional control; spreading rate control

INTRODUCTION

Mid-ocean ridge basalts (MORB) are arguably the most abundant igneous rocks on the Earth because they cover much of the global ocean floor and continue to form along the ~60 000 km long globe-encircling ocean ridges. They are also arguably the simplest igneous rocks on the Earth because they have relatively uniform chemical and isotopic compositions and because their origin is well understood as a straightforward consequence of plate tectonics; that is, plate separation induced passive mantle upwelling, decompression melting, melt extraction and cooling-dominated crustal-level differentiation (e.g. Klein & Langmuir, 1987; McKenzie & Bickle, 1988; Niu & Batiza, 1991*a*; Sinton & Detrick, 1992; Niu, 1997). Nevertheless, MORB compositional variations do exist on all scales and have been recognized from the early days of MORB studies (e.g. Sun *et al.*, 1975, 1979; Bryan & Moore, 1977; Langmuir & Hanson, 1980; Schilling *et al.*, 1983). The correlated large major element compositional variation has been correctly explained as resulting from low-pressure crustal-level differentiation (O'Hara, 1968*a*, 1968*b*; Walker *et al.*, 1979; Stolper, 1980; Perfit & Fornari, 1983; Christie & Sinton, 1986; Langmuir *et al.*, 1986; Langmuir, 1989; Sinton *et al.*, 1991; Sinton & Detrick, 1992; Batiza & Niu, 1992; Rubin *et al.*, 2009; O'Neill & Jenner, 2012; Coogan & O'Hara, 2015). Variations in abundances and ratios of incompatible elements and radiogenic isotopes have been logically interpreted as reflecting fertile mantle source compositional variation (e.g. Frey *et al.*, 1974; Sun *et al.*, 1975, 1979; Zindler *et al.*, 1984; Mahoney *et al.*, 1994; Niu *et al.*, 1996, 1999, 2001; Castillo *et al.*, 1998, 2000).

In addition to these repeatedly verified and generally accepted interpretations, MORB melts, in particular their major element compositions, are predicted also to carry information on both mantle sources and processes as shown by the correlated variations among major element abundances, incompatible element ratios and radiogenic isotopes (e.g. Langmuir & Hanson, 1980; Christie & Sinton, 1986; Natland, 1989; Niu & Batiza, 1991*a*, 1997; Mahoney *et al.*, 1994; Shen & Forsyth, 1995; Niu *et al.*, 1996, 1999, 2001, 2002*a*; Lecroart *et al.*, 1997; Rubin *et al.*, 2009) and by experimental petrology (e.g. Jaques & Green, 1980; Green & Falloon, 1998, 2005, 2015; Green, 2015). On the basis of ample observations and many studies, it is reasonable to state that MORB major element compositional variation must be inherited from the fertile mantle source compositional variation while also recording the physical conditions of magma generation as a result of plate spreading rate variation (Niu & Hékinian, 1997*a*, 1997*b*) and possibly mantle potential temperature variation (see Niu *et al.*, 2001). In this regard, the work by Klein & Langmuir (1987), after Dick *et al.* (1984), offered an unprecedented insight. It showed correlated variations of MORB Fe_8 and Na_8 (i.e. FeO and Na_2O values corrected for fractionation to a constant MgO value of 8 wt %) with ridge axial depth on a global scale. These correlations have been interpreted, following the experimental data of mantle peridotite melting (Jaques & Green, 1980), as reflecting varying extent and pressure of mantle melting in response to mantle solidus temperature variation of up to 250 K on a global scale. Langmuir *et al.* (1992) further elaborated quantitatively that the global MORB Fe_8 variation can be effectively used to calculate the mantle solidus temperature ($T_{[solidus]}$) and pressure ($P_{[solidus]}$) and mantle potential temperature (T_P) from the single MORB Fe_8 parameter: $P_{[solidus]} = 6{\cdot}11Fe_8 - 34{\cdot}5$ (kbar), $T_{[solidus]} = 1150 + 13P_{[solidus]}$ (°C), and hence $T_P = T_{[solidus]} - P_{[solidus]} \times 1{\cdot}8$ (°C) by using the experimentally determined dry mantle solidus curve and by assuming an adiabatic thermal gradient of 1·8 K kbar^{-1} (see McKenzie & Bickle, 1988; also see Niu & O'Hara, 2008).

Because of its convenience, Fe_8 has been popularly and axiomatically used in basalt studies. Given the well-documented mantle compositional heterogeneity for all major elements including FeO (e.g. Langmuir & Hanson, 1980; Niu *et al.*, 1999, 2002a), and to conscientiously inform readers of the inevitable errors when indiscriminately using Fe_8 in MORB studies, Niu & O'Hara (2008) demonstrated in detail in terms of straightforward petrological concepts, physical principles and logical arguments that Fe_8 is a misguiding parameter and cannot be used to infer mantle conditions and processes. In defence of the 'usefulness' of Fe_8, Langmuir and his group recently published two papers (Dalton *et al.*, 2014; Gale *et al.*, 2014) to refute the demonstrations by Niu & O'Hara (2008).

In commemoration of Michael J. O'Hara in this thematic O'Hara volume, and given the fundamental importance of understanding MORB petrogenesis as the foundation for igneous petrology in particular and global mantle dynamics in general, there is a pressing need to demonstrate explicitly and objectively that using Fe_8 in MORB studies can be misleading and must be treated with caution. The first-order global MORB major element compositional variation is largely source inherited and the signal of varying extent of melting as a function of plate spreading rate variation is also conspicuous as demonstrated previously (Niu & Hékinian, 1997*a*). A more comprehensive and thorough demonstration on

the origin of global MORB chemical systematics will be presented elsewhere.

THE PROBLEMS OF THE Fe_8 PARAMETER

Fe_8 is inappropriate in discussing mantle conditions and processes

It is logical to use basaltic melts in equilibrium with mantle mineralogy (e.g. olivine) to infer mantle melting conditions and processes. This requires that the melt have Mg# [$=Mg/(Mg+Fe^{2+})$] $\geq 0{\cdot}72$ to be in equilibrium with mantle olivine with Fo content [$Mg/(Mg+Fe)$] $\geq \sim 0{\cdot}90$ (or Fo_{90}) because of the well-established olivine–melt partitioning relationship $Mg\# = 1/[(1/Fo-1)/Kd+1]$, where $Kd = 0{\cdot}30 \pm 0{\cdot}03$ at low pressure (Roeder & Emslie, 1970) or higher values under mantle melting conditions with primitive MORB compositions (~10–15 wt % MgO; $Kd \approx 0{\cdot}32$; Baker & Stolper, 1994) or primitive ocean island basalt (OIB) compositions (~15–25 wt % MgO; $Kd \approx 0{\cdot}34$; Matzen *et al.*, 2011).

In Fig. 1 the Klein & Langmuir (1987) data show that the MORB melts with varying Fe_8 values have Mg# ~0·55–0·68, which is significantly lower than the Mg# $\geq 0{\cdot}72$ required to be in equilibrium with mantle olivine. Hence, in terms of the straightforward petrological concept, Fe_8 cannot be used to infer mantle processes simply because it records dominantly the highly evolved signature of MORB melts that have ascended across the Moho and left the mantle. The mantle solidus temperatures ($T_{[solidus]}$) and potential temperatures (T_P) calculated by using Fe_8 following Klein & Langmuir (1987) and Langmuir *et al.* (1992) thus have no significance. The varying low Mg# values exhibited by MORB melts with varying Fe_8 (as in Fig. 1) are consistent with varying extents of crustal-level MORB melt evolution (O'Hara, 1968*a*, 1968*b*; Walker *et al.*, 1979; Niu, 1997).

In this context, it is important to note that the popular emphasis on mantle pyroxenites as sources of OIB and some alkali basalts (e.g. Sobolev *et al.*, 2007) has led some to consider that mantle melts generated by pyroxenite melting should have low Mg# (e.g. Yang & Zhou, 2013). This is wrong in concept and incorrect in practice, for the following reasons: (1) melting of pyroxenites with Mg# $\geq 0{\cdot}90$ would still produce primitive melts with Mg# $\geq 0{\cdot}72$ constrained by the Fe–Mg exchange Kd (i.e. $Kd^{clinopyroxene/melt} \approx Kd^{orthopyroxene/melt} \approx Kd^{olivine/melt} \approx 0{\cdot}30 \pm 0{\cdot}03$ (e.g. Grove *et al.*, 1992; Niu *et al.*, 2002*b*); (2) partial melts of pyroxenites with low Mg# values (e.g. subducted ocean crust) will readily reach chemical equilibrium with the ambient mantle mineralogy to gain Mg# $\geq 0{\cdot}72$, because pyroxenites are volumetrically minor; (3) the melts generated by pyroxenite total melting will have the same Mg# as the pyroxenites and will again reach equilibrium with the ambient mantle mineralogy to gain Mg# $\geq 0{\cdot}72$, regardless of the actual pyroxenite compositions. Hence, ascending mantle melts prior to crossing the Moho should all be in equilibrium with mantle mineralogy and have Mg# $\geq 0{\cdot}72$ unless

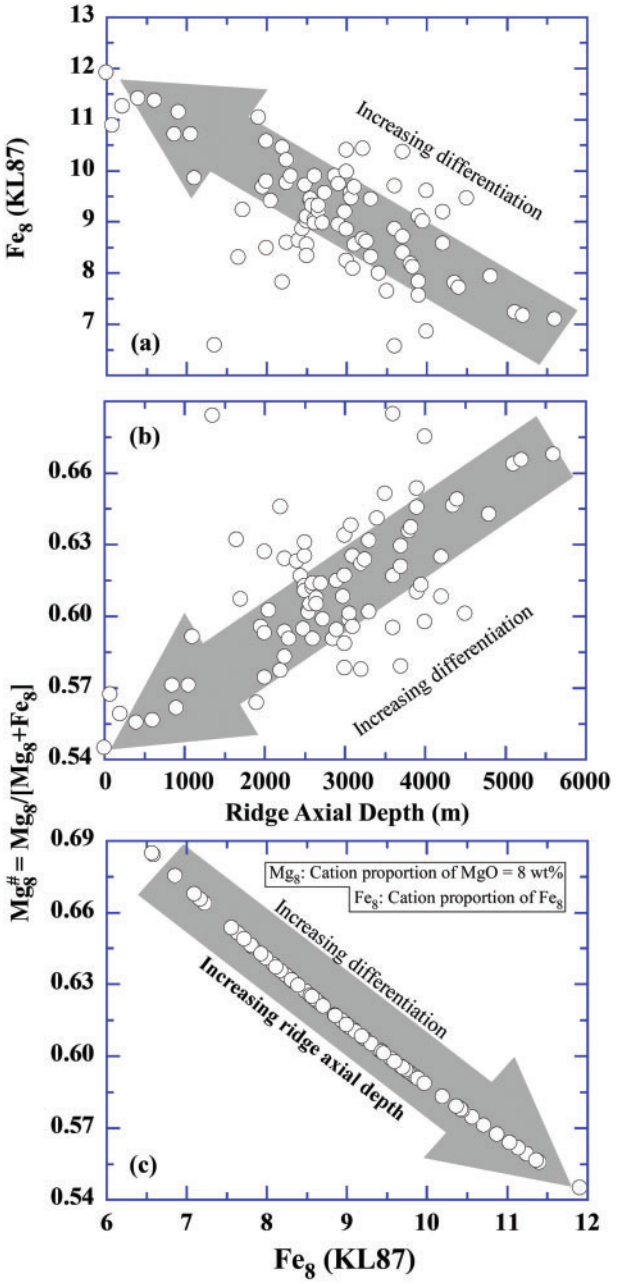

Fig. 1. (a) Location-averaged global MORB data of Klein & Langmuir (1987) (KL87) indicating the first-order MORB major element Fe_8 variation (weight per cent FeO corrected for fractionation effect to MgO = 8·0 wt %) as a function of ocean ridge axial depth (water depth). Klein & Langmuir used Fe_8 to infer mantle temperature variation (see Langmuir *et al.*, 1992). Niu & O'Hara (2008) demonstrated that this Fe_8 usage is erroneous because to reveal mantle melting conditions and processes, MORB melts must have $Mg\# = Mg/(Mg+Fe^{2+})$ (10% total Fe is assumed to be Fe^{3+} in the Mg# calculation) $\geq 0{\cdot}72$ to be in equilibrium with mantle olivine of Fo ≥ 90. However, MORB Fe_8 values correspond to Mg# = 0·54–0·68 as in (b), which are too evolved to be in equilibrium with mantle olivine and thus cannot be used to infer mantle melting conditions and processes, but largely tell us about crustal-level differentiation processes. (c) combines (a) and (b) to illustrate the variably evolved nature of MORB melts corrected to Fe_8. This figure is simplified from Niu & O'Hara (2008).

significant cooling and olivine crystallization has taken place during melt ascent through the cold thermal boundary layer beneath ridges (or lithospheric mantle elsewhere) as seen in abyssal peridotites (Niu, 1997; Niu *et al.*, 1997). Therefore, if one wants to unmistakably decipher mantle processes from MORB major element compositions, it is required to correct for the effects of crustal-level processes to Mg# $\geq$ 0·72 (e.g. Si_{72}, Ti_{72}, Al_{72}, Fe_{72}, Mg_{72}, Ca_{72} and Na_{72}), which must be constrained by the most primitive MORB glass samples with Mg# $\geq$ 0·72 (see Niu *et al.*, 1999; Niu & O'Hara, 2008).

The Klein & Langmuir (1987) correction to Fe_8 has no significance

Figure 2 is modified from Niu & O'Hara (2008) to compare the fractionation-corrected data of Klein & Langmuir (1987) with fractionation-uncorrected average MORB data with MgO $\geq$ 7 wt %. This illustrates that the apparently meticulous correction procedure of Klein & Langmuir (1987) is an unnecessary data manipulation because the corrected Fe_8 and Na_8 values have no geological difference from the uncorrected data. This is true for Na_2O and largely true also for FeO and Mg# because the Klein & Langmuir (1987) interpretations were largely based on the large range (i.e. in Fe_8) defined by samples from the shallowest and deepest ridges (see Niu, 1997). This evident problem remains despite the apparently exhaustive arguments in defence of the Fe_8 parameter by Gale *et al.* (2014) as discussed below.

The Gale *et al.* (2014) justification of Fe_8 correction is unjustified

Gale *et al.* (2014) made a commendable effort in providing an updated MORB dataset for improved studies. They discussed global MORB systematics and their origin. However, the very heart of the study by Gale *et al.* (2014) is to refute the Niu & O'Hara (2008) criticism against using Fe_8 and to defend the Fe_8-based interpretations by Klein & Langmuir (1987) and Langmuir *et al.* (1992). The Niu & O'Hara (2008) criticism of using Fe_8 has three specific points: (1) Fe_8, representing highly and variably evolved MORB compositions, cannot be used to decipher mantle processes as discussed above; (2) MgO and FeO are both sensitive and proportional to the pressure of melting in primitive melts in equilibrium with mantle mineralogy (see Niu & O'Hara, 2008, fig. 1), but the use of the Fe_8 parameter with constant MgO = 8 wt % has ignored MgO as a potential pressure indicator; (3) SiO_2 is also sensitive to pressure of melting, but is inversely proportional to MgO and FeO in primitive melts in equilibrium with mantle mineralogy (see Niu & O'Hara, 2008, fig. 12a), but MORB SiO_2 shows no pressure signature (see Niu & O'Hara, 2008, fig. 12b and c). Gale *et al.* (2014) skilfully replied to these critical points through an apparently painstaking effort, which is in fact unjustified and has an additional misguiding effect.

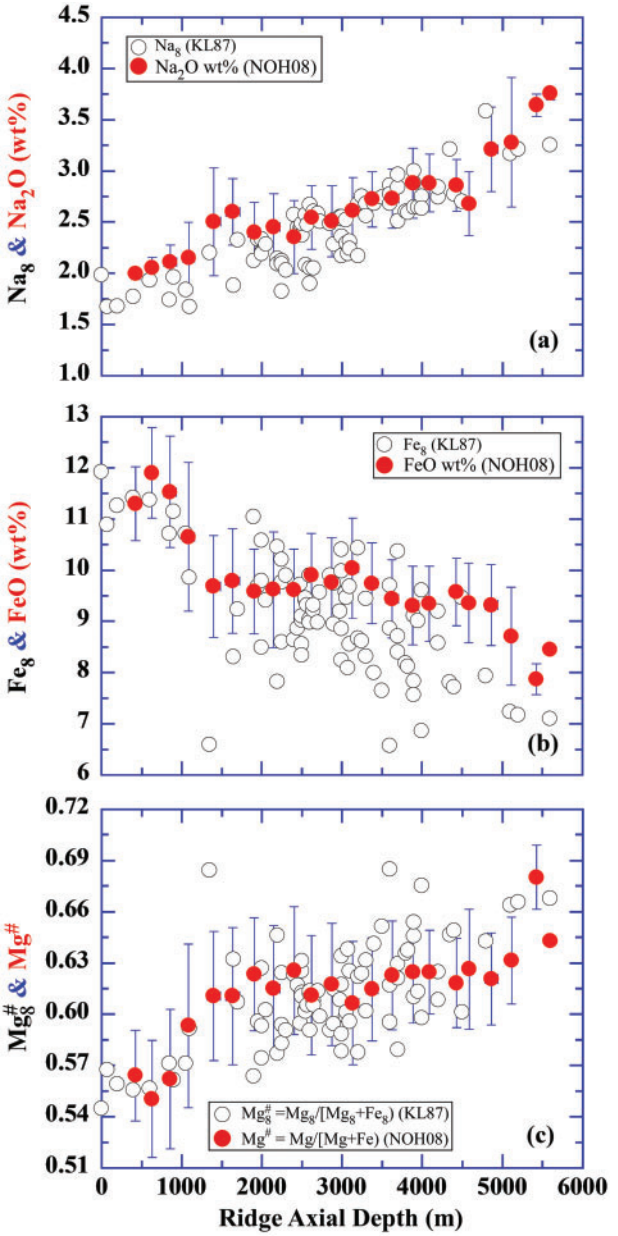

Fig. 2. Comparison of location-averaged global MORB Na_8 (a), Fe_8 (b) and Mg# (c) [calculated from (b)] with uncorrected depth-interval averages of Na_2O, FeO and Mg# for samples with MgO > 7·0 wt % from Niu & O'Hara (2008) (NOH08) to show that the apparently meticulous correction procedure of Klein & Langmuir (1987) (KL87) has little significance because both corrected and uncorrected data are essentially the same, dominated by a variably evolved nature with Mg# = 0·54–0·68. This figure is simplified from Niu & O'Hara (2008), where details of depth-interval averages are explained in their fig. 3 and accompanying text.

The Gale *et al.* (2014) global MORB data in the MgO–FeO space are illustrated in Fig. 3a. It is evident that the corrected Fe_8 values must be equal to or greater than the range of 7–12·5 (~5·5 Fe units) as indicated for FeO at MgO = 8 wt %. To argue for Fe_8 to be useful in reflecting mantle-melting conditions as claimed, Gale *et al.* (2014) also corrected MORB melts to be in equilibrium with mantle olivine of Fo_{90}, denoted as Fe_{90}. As shown

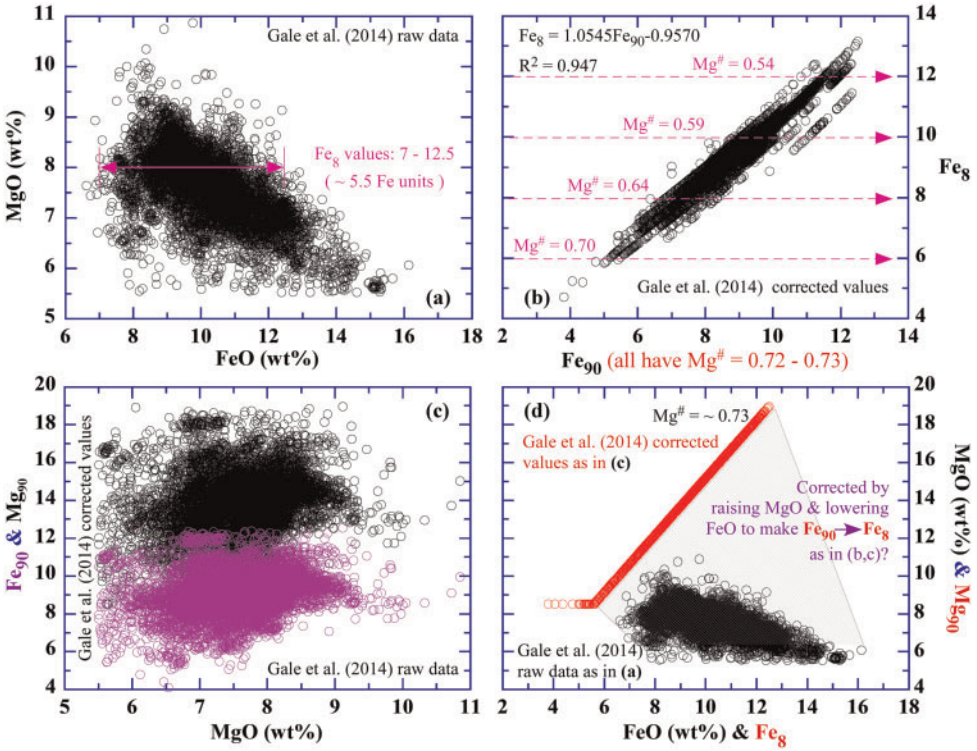

Fig. 3. (a) MgO–FeO covariation plotted using the Gale *et al.* (2014) MORB dataset, in which the concept of Fe_8 is shown by FeO values at MgO = 8 wt % as indicated. (b) The essentially identical Fe_8 and Fe_{90} values and ranges calculated by Gale *et al.* (2014) were used to make the case that MORB compositions with Fe_8 are the same as MORB Fe_{90} and thus should be in equilibrium with mantle olivine of Fo_{90}. However, this is not true because Mg# = *f*(MgO = 8, Fe_8) ~ 0·54–0·70, variably and significantly lower than Mg# = 0·72 as indicated, showing that $Fe_8 = Fe_{90}$ is conceptually contradictory in terms of elementary petrology. (c) Plot of MgO against Mg_{90} and Fe_{90} from Gale *et al.* (2014), revealing that the Fe_{90} values were calculated by adding olivine to each MORB sample until $Fe_{90} \rightarrow Fe_8$, hence obtaining the same Fe_8 and Fe_{90} as in (b); this procedure involves adding as much MgO as required (on average a factor of two; i.e. Mg_{90} vs MgO along the horizontal axis), while lowering FeO as needed [lower mean and range of Fe_{90} than actual FeO in (a)]. (d) Comparison of raw data as in (a) with Gale *et al.* (2014) calculated Fe_8 (the same as Fe_{90}) and Mg_{90} in MgO–FeO space, revealing that the Gale *et al.* (2014) calculated Fe_8(≈Fe_{90})–Mg_{90} values (heavily overlapped open red circles) are remote from the actual data, beyond the petrologically permitted interpolation and extrapolation range. Thus, the Gale *et al.* (2014) Fe_{90}–Mg_{90} values and ranges have no relevance to the actual data.

in Fig. 3b their calculated Fe_8 and Fe_{90} are essentially the same, with the calculated Fe_8 (or Fe_{90}) in the range of 6–13 (~7 Fe units). The significant Fe_8–Fe_{90} correlation with the same range of values looks convincing, but is curiously incomprehensible. It is puzzling and confusing why MORB melts are in equilibrium with mantle olivine Fo_{90} if expressed with Fe_{90} (i.e. horizontal-axis $Mg\#^{melt}$ ~0·72–0·73), whereas these same MORB melts are not in equilibrium with mantle olivine if expressed with Fe_8 (i.e. vertical-axis $Mg\#^{melt}$ ~0·70 $-<$ 0·54) despite the simple fact that $Fe_8 \approx Fe_{90}$ (Fig. 3b). I leave this petrological impossibility to readers to comprehend, but only offer my personal understanding of the Gale *et al.* (2014) correction in terms of a simple mathematic treatment.

It is obvious that the only way to produce the correlated values in Fig. 3b is to set a given Fe_8 value as the target to produce $Fe_{90} \rightarrow Fe_8$. This can be done by raising MgO while lowering FeO as much or as little as needed. This is illustrated in Fig. 3c, where MgO must be raised, on average, by a factor of two (e.g. Mg_{90}) higher than the actual data (the horizontal-axis values), whereas FeO must be lowered from the range of 7–16 (horizontal-axis value of Fig. 3a) to Fe_{90} ~5–12 (Fig. 3c). This may be assumed to be equivalent to adding olivine Fo_{90} (or other Fo values) until $Fe_{90} \approx Fe_8$, by adding more olivine (hence more MgO) to samples with higher Fe_8 and less olivine (hence less MgO) to samples with lower Fe_8. In doing so, the primary melt in the mantle source region parental to each of the MORB samples would have Mg# ~0·72–0·73 in equilibrium with the mantle mineralogy (see Fig. 3d).

There has been a long history in petrology of adding olivine to evolved basaltic melts to infer their primary magma compositions in equilibrium with the mantle mineralogy. Despite the various uncertainties in doing so, this is nevertheless a useful approach. The question is if this approach by Gale *et al.* (2014) is appropriate here. The answer is simply 'No' because (1) adding varying amounts of olivine with the purpose of making $Fe_{90} \rightarrow Fe_8$ is an unjustified exercise, and (2) the so calculated FeO (Fe_{90}, same as Fe_8) and MgO (Mg_{90}) in equilibrium with mantle olivine of Fo_{90} shown by the stacked red open circles with large MgO (~8–19 wt %) and FeO (~6–12 wt %) variations (Fig. 3d) are remotely removed from, and having no relevance to, the actual

data (the black open circles with MgO $\sim\leq$ 10·5 wt %). That is, the Gale *et al.* (2014) correction to Fe_{90} is entirely unconstrained and is petrologically unlikely - way beyond the data and beyond petrologically possible and permitted interpolation and extrapolation range.

Their 'olivine addition' procedure apparently answered the criticisms by Niu & O'Hara (2008) (see above) because olivine controls the positive Fe_{90}–Mg_{90} correlation (red circles in Fig. 3d) and negative Si_{90}–Mg_{90} and Si_{90}–Fe_{90} correlations (not shown here) as if the varying Fe_{90}, Mg_{90} and Si_{90} values were consistent with mantle melting pressure effects. It is objectively correct to state that MORB melts preserve no melting pressure signature at all in terms of SiO_2 as demonstrated in fig. 12 of Niu & O'Hara (2008) [also see Niu *et al.* (2011) and further illustration below]. The correlated Fe_{90}–Mg_{90}–Si_{90} variations by Gale *et al.* (2014) have no pressure significance, but are the artefact of making $Fe_{90} \rightarrow Fe_8$ (Fig. 3b).

THE EFFICACIES OF MORB MAJOR ELEMENTS AT Mg# = 0·72

About Mg# ≥ 0·72 and MORB melt compositions at Mg# = 0·72

Basaltic melts having Mg# ≥ 0·72 do not constrain mantle solidus conditions (i.e. P_o and T_o) because Mg# = *f*(MgO, FeO). A primitive MORB melt with MgO = 10·5 wt % and FeO = 8·1 wt % gives Mg# ~0·72 (assuming 90% total Fe as Fe^{2+}) and a primitive ocean island basaltic melt erupted on thickened lithosphere with MgO = 18 wt % and FeO = 13·9 wt % can also give Mg# ~0·72 (Niu *et al.*, 2011). However, variations of MORB melt compositions corrected to Mg# = 0·72 (i.e. Fe_{72} and Mg_{72} as well as Si_{72}, Ti_{72}, Al_{72} Ca_{72} and Na_{72}) can be used to discuss mantle sources and processes because primitive melts having Mg# ≥ 0·72 are in equilibrium with mantle olivine of Fo ≥ 0·90 (Fo_{90}).

However, MORB melt FeO contents corrected to MgO = 8 wt % (i.e. Fe_8 with Mg# = 0·56–0·68) are too evolved to be in equilibrium with mantle olivine and cannot be used to discuss mantle processes as elaborated above. The Gale *et al.* (2014) corrected Fe_{90} cannot be used either because $Fe_{90} = Fe_8$ (Fig. 3b).

Petrological effectiveness of Fe_{72} versus misguiding Fe_8

Gale *et al.* (2014) asserted that their new data are not in agreement with the presentation of Niu & O'Hara (2008), 'whose results relied on an inaccurate fractionation correction procedure, which led them to large errors for high- and low-FeO magmas' (p. 1051). This is an incorrect statement as further demonstrated below in terms of basic petrological concepts and elementary illustrations.

Figure 4a is a familiar diagram showing global MORB melt (glass) major element oxide abundance variations as a function of MgO. Because MgO is

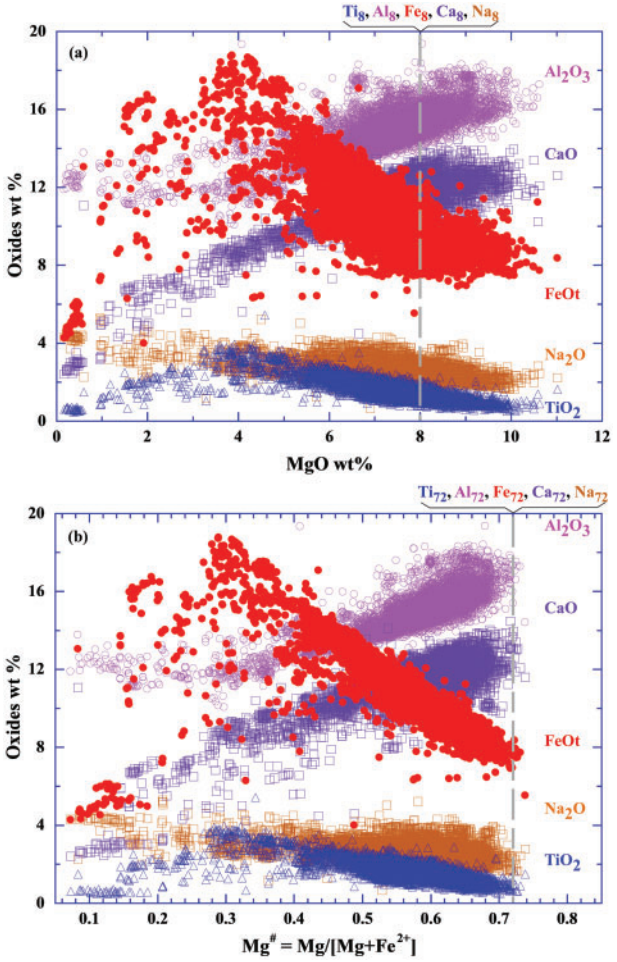

Fig. 4. (a) Global MORB major element oxides [TiO_2, Al_2O_3, FeOt (where t indicates total Fe expressed as FeO), CaO and Na_2O] abundance variations as a function of MgO (data from PETDB database: www.petdb.org). (b) As in (a), but plotted as a function of Mg# [Mg/(Mg + Fe^{2+}), assuming Fe^{2+}/total Fe = 0·9 for simplicity]. As MgO is linearly proportional to the liquidus temperature (e.g. Weaver & Langmuir, 1990; Danyushevsky, 1998; Niu *et al.*, 2002*b*; Niu & O'Hara, 2009), all the oxide variations with decreasing MgO define first-order liquid lines of descent (LLD) during cooling-dominated MORB melt cooling and evolution. In detail, however, these trends are not simple LLD, but the combined effect of LLD, magma mixing, melt–rock reactions and complex open-magma chamber processes (O'Hara, 1977). In other words, these trends are the net effect of all these natural processes. Mg# is not strictly linearly proportional to the liquidus temperature, but is convincingly close for MORB melts with MgO > ~ 4 wt % (see Niu *et al.*, 2002*b*; Stone & Niu, 2009), with deviation caused by varying FeO content. Hence, to a first order, MORB major element oxide abundance variations versus Mg# in (b) are also a net effect of the combined MORB melt evolution trends. As indicated by the vertical gray dashed lines, the band width for each oxide would be the values and ranges at MgO = 8·0 wt % in (a) or at Mg# = 0·72 in (b), respectively.

proportional to the liquidus temperature, the data trend for each of the oxides with decreasing MgO is to a first order consistent with the liquid line of descent (LLD), which is conceptually the residual melt compositional variation as the result of fractional crystallization of olivine + spinel → plagioclase + olivine → plagioclase +

clinopyroxene ± olivine prior to reaching MgO ~4·0 wt %, after which crystallization of titanomagnetite (Ti–Fe oxides) depletes FeO and TiO_2 while increasing SiO_2, entering the basaltic-andesite stage of basaltic magma evolution (e.g. Niu *et al.*, 2002*b*; Niu, 2005*a*; Niu & O'Hara, 2009; Stone & Niu, 2009). Strictly speaking, the data trends in Fig. 4a are not simple LLD, but the net effect of cooling-dominated crustal-level processes combined (e.g. fractional crystallization, magma mixing, melt–rock assimilation and, or, reaction and other aspects of complex open-magma chamber processes). The Klein & Langmuir (1987) and Langmuir *et al.* (1992) method of calculating Fe_8 and Na_8 was to assume a common LLD slope for FeO–MgO and Na_2O–MgO, respectively, to project individual data points onto the plane of MgO = 8 wt % as indicated, by back-tracking (for samples with MgO < 8 wt %) and forward-tracking (for samples with MgO > 8 wt %). To avoid correction errors, Klein & Langmuir (1987) and Langmuir *et al.* (1992) chose samples with MgO ≥ 5·5 wt %. One can do the same to obtain Ti_8, Al_8, Ca_8 and Ca_8/Al_8 (Niu & Batiza, 1991*a*, 1993, 1994). The only difference of the Gale *et al.* (2014) approach from that of Klein & Langmuir (1987) and Langmuir *et al.* (1992) was to obtain separate sets of LLD for MORB samples from each ridge segment with the belief that samples from different ridge segments have different LLD trends as discussed by Niu & Batiza (1993). This philosophical consideration is reasonable, but has unavoidable problems: (1) MORB samples from most ridge segments do not have enough MgO variation coverage to obtain suitable LLD (if they were LLD); hence, assumptions must be made to justify the chosen LLD slopes that in practice cannot be constrained; (2) natural MORB sample suites do not define pure LLD, but show the combined effects of complex crustal-level processes (see above).

The same data as a function of Mg# are plotted in Fig. 4b. The data trends are again not simple LLD, but the net effect of compound crustal-level processes (see above). To correct for such net effect for the global dataset, it is logical to find a common set of correction coefficients for each oxide, applicable to the global dataset in this Mg# variation diagram. Obviously, the most objective, logical and simplest method is to obtain a set of polynomial regression coefficients for each oxide based on the entire global dataset (see Niu *et al.*, 1999; Niu & O'Hara, 2008) and to project each sample along the polynomial curves to Mg# = 0·72 as indicated by the vertical gray dashed line in Fig. 4b. To avoid unnecessary errors, Niu & O'Hara (2008) used MORB samples with MgO ≥ 7·0 wt %, thus the polynomial coefficients mostly give rise to linear coefficients, especially for FeO and MgO [see Appendix of Niu & O'Hara (2008)]. This method of correction is objective, logical and simple for the following reasons.

1. We follow the data (Fig. 4b) without making any unnecessary assumption that cannot be justified.
2. Regardless of how evolved and how complex the histories each MORB sample may have experienced through crustal-level processes, its parental melt must have once had Mg# ≥ 0·72 within the range constrained by the data as indicated by the gray dashed line at Mg# = 0·72 (Fig. 4b).
3. The method corrects for the net effect of compound crustal-level processes expressed by the global data trends without having to know exactly what LLD for a single sample suite may be (Fig. 4b).
4. Mg# = 0·72 is the best reference point: (a) the most primitive MORB samples have Mg# ≈ 0·72–0·73 (corresponding to some of the samples with MgO ≈ 10·5 wt % in Fig. 4a) so that the correction is well constrained within the known dataset (Fig. 4b) without having to make assumptions that cannot be justified; (b) Mg# = 0·72 is about the minimum value for a basaltic melt required to be in equilibrium with mantle olivine.
5. The key difference of the Niu & O'Hara (2008) correction method is not an 'inaccurate fractionation procedure' as incorrectly stated by Gale *et al.* (2014), but the use of the petrologically and logically best reference of Mg# = 0·72 (Fig. 5b) rather than the problematic reference of MgO = 8·0 wt % (Fig. 5a).

We should note that correction to MgO = 8 wt % or Mg# = 0·72 has less effect on the relative abundances and systematics of Ti_{72} (vs Ti_8), Al_{72} (vs Al_8), Ca_{72} (vs Ca_8) and Na_{72} (vs Na_8), as well as Ca_{72}/Al_{72} (vs Ca_8/Al_8), but has large effects on Fe_{72} (vs Fe_8) and Mg_{72} (vs $Mg_8 = 8$) because of the FeO–MgO–Mg# interrelationships as further illustrated below.

More on the effectiveness of Fe_{72} versus misguiding Fe_8 (and Fe_{90})

The variation of FeOt against MgO and Mg# respectively (Fig. 5a and b) explicitly shows that Fe_{72} is objective and more logical than Fe_8, and why Fe_{72} values must have a significantly smaller range (~1·0 Fe unit) than Fe_8 (~4·5 Fe units) without any correction. With decreasing MgO (or Mg#), the upper bound of FeOt reaches the maximum at MgO ≈ 4 wt % (or Mg# ≈ 0·30) as a result of combined fractional crystallization of spinel + olivine + plagioclase + clinopyroxene before Fe–Ti oxide (titanomagnetite) appears on the liquidus at MgO ≤ ~4 wt % to cause FeOt depletion. By considering samples with MgO > 5·5 wt % only, this can certainly avoid potential errors caused by highly evolved samples in correcting to Fe_8 (Klein & Langmuir, 1987; Langmuir *et al.*, 1992; Gale *et al.*, 2014). However, the actual data, with no correction, show that at MgO = 8 wt %, FeO = Fe_8 ~7·2 – ~11·7 wt % has an Fe_8 range of ~4·5 Fe units as indicated (Fig. 5a). This is the very minimum Fe_8 spread because correction for samples with MgO > 5·5 wt % and < 8·0 wt % onto the MgO = 8·0 wt % plane can only make the Fe_8 spread larger (i.e. > ~4·5 Fe units). On the other hand, it is evident that FeO at or projected to Mg# = 0·72 has a limited variation of

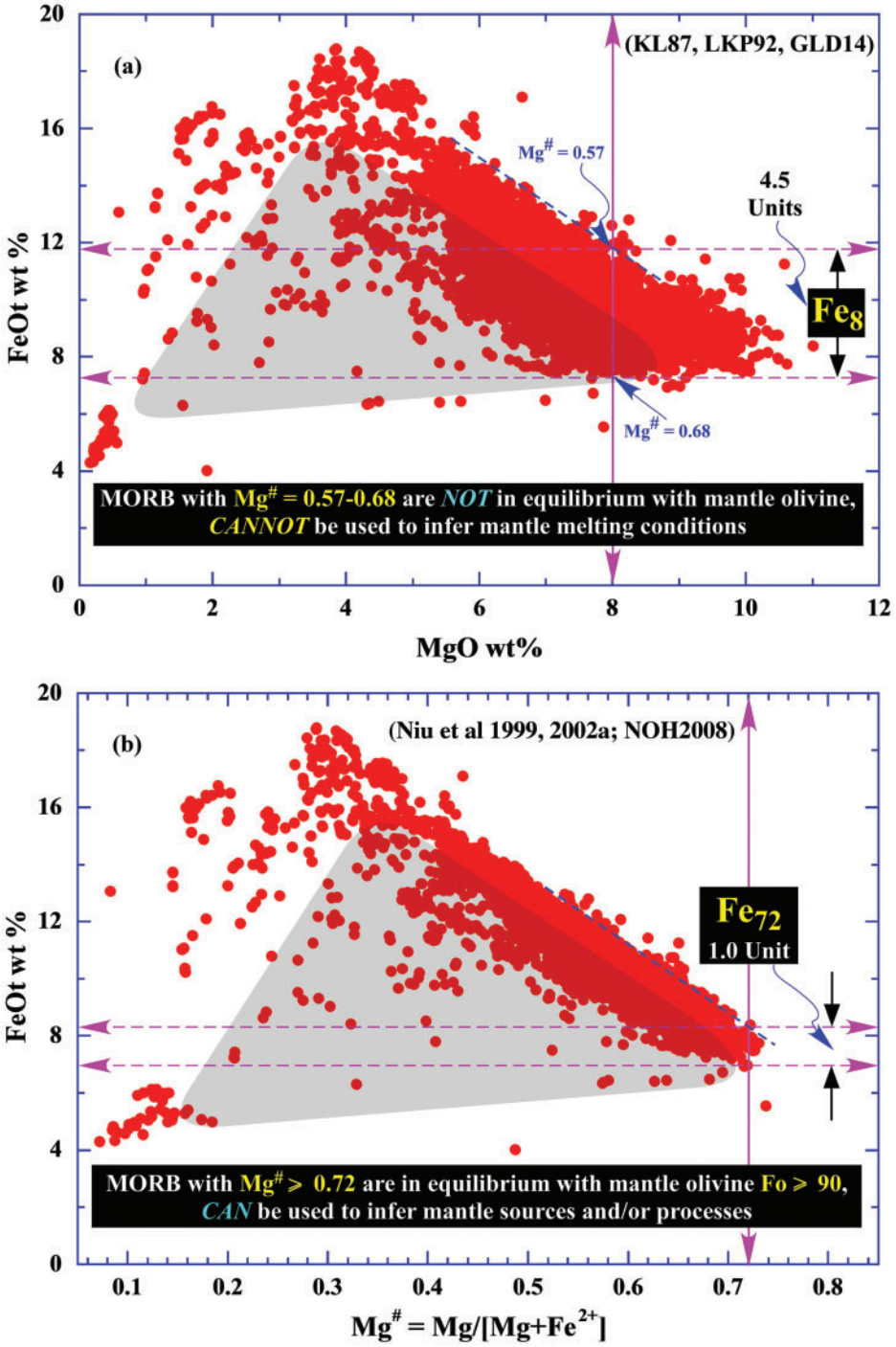

Fig. 5. The same two panels as in Fig. 4, but only FeOt is plotted to highlight the difference between Fe_8 (a) and Fe_{72} (b). The maximum of the FeOt upper bound at MgO ~4 wt % in (a) is to a first order consistent with a liquid line of descent resulting from the combined effects of fractional crystallization of spinel + olivine + plagioclase + clinopyroxene before Fe–Ti oxide (titanomagnetite) on the liquidus at MgO ≤ ~4 wt %. Klein & Langmuir (1987) (KL87), Langmuir *et al.* (1992) (LKP92) and Gale *et al.* (2014) (GLD14) used samples with MgO ≥ 5·5 wt % and Niu & O'Hara (2008) (NOH2008) used samples with MgO ≥ 7·0 wt %, so the obviously scattered FeO values below these chosen cut-off MgO values will not affect the calculated Fe_8 or Fe_{72}. However, those samples below the main trend in the broad shaded region cannot simply be evolved MORB melts, but are most consistent with being 'snapshots' of magma mixing in open magma chamber (or something equivalent) systems, largely resulting from mixing of newly replenished primitive melts with already highly evolved melts having low MgO and low FeO. There is no doubt that many samples towards the lower bound of the main data band at a given MgO or Mg# have resulted from such mixing, although it is not possible to precisely quantify this process. It is reasonable to infer that such mixing is more obvious in FeO–MgO space (a) than in the FeO–Mg# space (b) because of the significantly fatter lower bound at a given MgO in (a). The key message here is as follows: for this same dataset, Fe_8 ~7–11·5 wt % with variation of ~4·5 Fe units, corresponding to Mg# = 0·68 – 0·57, far too evolved to be used for discussing mantle melting conditions and processes. On the other hand, Fe_{72} ~7–8·0 wt % with ~1·0 Fe unit variation at a constant Mg# = 0·72, which is in equilibrium with mantle olivine of Fo_{90} and thus can be logically used to discuss mantle melting conditions and processes. It is straightforward that the small Fe_{72} range of ~1 Fe unit [versus the large Fe_8 range of >4·5 Fe units found by Gale *et al.* (2014)] is a property of the actual data, and is not the result of an inaccurate correction procedure as incorrectly stated by Gale *et al.* (2014).

~7–8 wt % with an Fe_{72} range of ~1 Fe unit as illustrated. Given the narrow FeO band at a given Mg#, and because all the samples, regardless of how they evolved, were modified through complex crustal-level processes, their parental melts must have once passed through Mg# = 0·72 with an Fe_{72} spread that cannot be significantly greater than that observed. This is a straightforward demonstration based on the actual data without applying any correction, in contradiction to the incorrect statement by Gale *et al.* (2014).

In summary, the data, not the correction procedure, demonstrate that Fe_8 ~7·2 – ~11·7 wt % with a large range of ~4·5 Fe units (Fig. 5a; Klein & Langmuir, 1987; Langmuir *et al.*, 1992; Gale *et al.*, 2014). Also the data, not correction procedure, demonstrate that Fe_{72} = ~7·0 – ~8·0 wt % with a small range of ~1 Fe unit (Fig. 5b; Niu & O'Hara, 2008). This 'coincidence' of the actual FeO at Mg# = 0·72 with Fe_{72} by Niu & O'Hara (2008) demonstrates the objective validity of the Niu & O'Hara (2008) correction procedure, which strictly follows basic petrological principles and the intrinsic structure within the data. Figure 6a objectively compares Fe_{72} (Niu & O'Hara, 2008) with Fe_8 (Klein & Langmuir, 1987; Langmuir *et al.*, 1992) in Na_2O–FeO space. Figure 6b and Fig. 6c are the same, but using the Gale *et al.* (2014) data to compare the Niu & O'Hara (2008) method (250 m ridge depth interval averages) with the 237 global ridge segment averages of Gale *et al.* (2014) (excluding the three averages from Iceland on land). It should be noted that Niu & O'Hara (2008) used 9130 MORB glass samples with MgO > 7·0 wt %, but there are only 7607 samples with MgO > 7·0 wt % and no data for the depth interval of 4750–5000 m in the Gale *et al.* (2014) dataset. Nevertheless, Fig. 6b (comparison of Na_{72} and Fe_{72} with Na_8 and Fe_8) and Fig. 6c (comparison of Na_{72} and Fe_{72} with Na_{90} and Fe_{90}) are essentially the same as Fig. 6a in terms of process interpretations. Therefore, the statement by Gale *et al.* (2014) against the Niu & O'Hara (2008) method is inappropriate, and has the effect of further misguidance in addition to the misleading Fe_8. The proposed large mantle potential temperature variation of ~250 K on the basis of the large Fe_8 range [and the same large Fe_{90} range obtained by the Gale *et al.* (2014) method] is manifestly an artefact. Therefore, any intended use of Fe_8 should be avoided in order to advance our genuine understanding of ocean ridge dynamics.

THE MEANING OF MORB MAJOR ELEMENTS AT Mg# = 0·72

We can now use MORB major element compositions at Mg# = 0·72 to infer mantle processes. Because ridge axial depth variation (~0 to ~6000 m) and plate spreading rate variation (<10 to >150 mm a^{-1}) are the only two largest known physical variables along the global ocean ridge system, our task is to examine whether MORB major element compositions respond to these two physical variables. Klein & Langmuir (1987) recognized Na_8 and Fe_8 correlations with ridge axial depth and Niu & O'Hara (2008) confirmed this but emphasized that

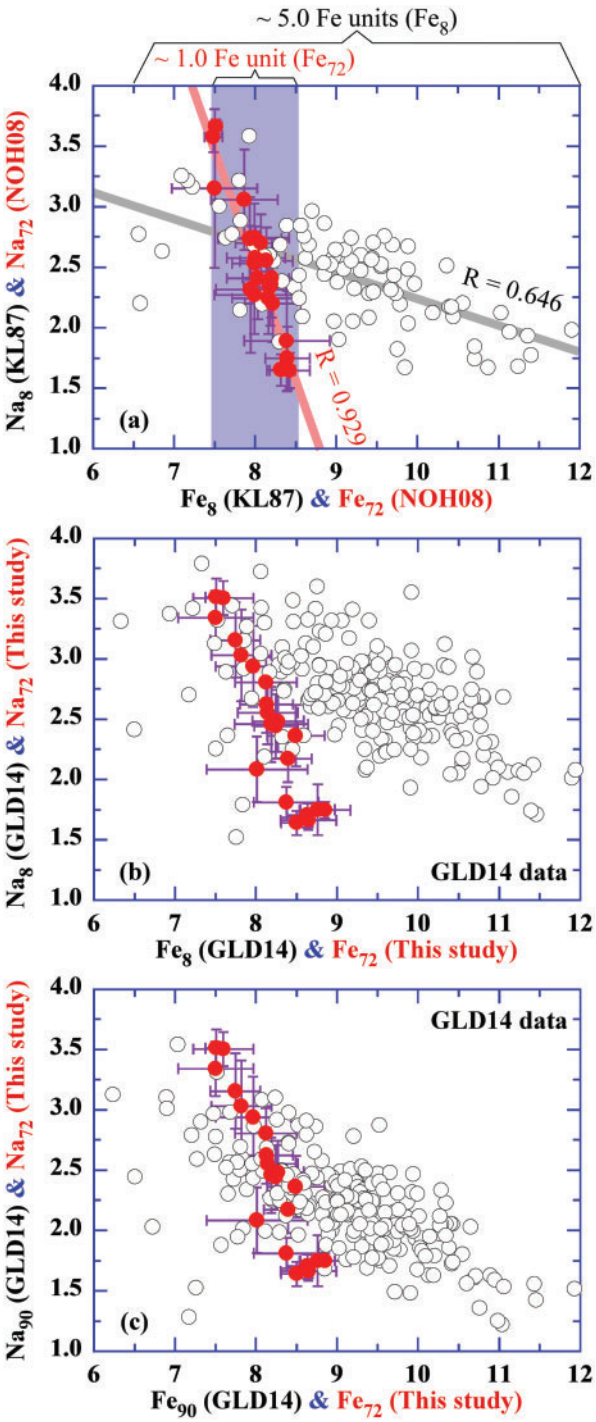

Fig. 6. (a) Comparison of Na_8–Fe_8 of Klein & Langmuir (1987) (KL87) with Na_{72}–Fe_{72} of Niu & O'Hara (2008) (NOH08). Na_8 and Na_{72} values and ranges are similar, which is obvious from Fig. 4, but Fe_8 and Fe_{72} are very different, with variations in Fe_8 ~ 5 units compared with Fe_{72} ~ 1 unit, which is rather obvious in Figs 4 and 5. This straightforward difference between Fe_8 and Fe_{72} as demonstrated by the actual data (Figs 4 and 5) is an intrinsic property of the data, but was incorrectly interpreted by Gale *et al.* (2014) as an effect of an erroneous or inaccurate fractionation correction procedure of Niu & O'Hara (2008). (b, c) As in (a), the same comparison of Na_{72}–Fe_{72} using the Gale *et al.* (2014) (GLD14) dataset with the Na_8–Fe_8 of Gale *et al.* (2014) (b) and Na_{90}–Fe_{90} from Gale *et al.* (2014) (c). Samples from Iceland and nearby ridges with seawater depths < 200 m are excluded.

Ti_{72}, Al_{72}, Mg_{72}, Ca_{72}, Ca_{72}/Al_{72} as well as Na_{72} and Fe_{72} all correlate with ridge axial depth and offered different explanations for the cause of such correlations. Niu & Hékinian (1997*a*) demonstrated the significant correlations of Al_8 and Ca_8/Al_{72} (also K_8/Ti_8 as shown below) with plate spreading rate, which, together with the then available global abyssal peridotite data, were interpreted to reflect the extent of mantle melting, which increases with increasing plate spreading rate as expected in terms of straightforward physics (Reid & Jackson, 1981; Niu & Hékinian, 1997*a*). However, Gale *et al.* (2014) denied the existence of such a correlation by stating: 'There is no correlation between the chemical parameters and spreading rate' (p. 1080). In this section, I discuss these correlations, but it is conceptually important first to clarify that spreading rate variation and ridge depth variation are two genetically unrelated variables (except for extremely slow-spreading ridges; see below) and we need to separate the effects of the two variables for a better understanding of ridge processes.

The origin of plate spreading rate variation and ridge axial depth variation

Plate spreading rate here refers to the separation rate of the two plates with respect to each other on both sides of the ridge, which is also called the 'full spreading rate' or 'total opening rate' of the ridge, and is determined by the absolute motion speeds of the two plates relative to some hotspot reference framework (e.g. DeMets *et al.*, 1990). The absolute motion speed of a given plate has been well understood as resulting from subducting slab pull (e.g. Forsyth & Uyeda, 1975; McKenzie & Bickle, 1988; Davies & Richards, 1992), which is straightforward to understand for plates connected with subduction zones such as those in the Pacific, but not so obvious for plate motion in the Atlantic. Nevertheless, Niu (2014, 2016) illustrated that (1) seafloor spreading in ocean basins with passive margins (e.g. the Atlantic type) and (2) continental drift are simply passive movements in response to trench retreat of active seafloor subduction in ocean basins like the Pacific with subduction zones. Hence, the varying speeds of plate motion determine the plate spreading rates of the ridges concerned. Because ocean ridge magmatism results from plate separation, it is expected that the effect of plate separation rate variation must be recorded in the MORB chemistry. To deconvolve the effect of plate spreading rate variation from the effects of all other probable or possible variables involves averaging MORB chemistry with respect to spreading rate intervals, so as to average out all other possible effects (Niu & Hékinian, 1997*a*). This is mathematically the same as seeking the partial derivatives of a quantity with respect to a particular variable, with all other variables held constant (Niu & O'Hara, 2008).

The above elaboration demonstrates that globally the large ridge axial depth variation is unrelated to spreading rate (see below for very slow spreading ridges). This is because ridge axial depth variation is largely controlled isostatically by sub-ridge material density variations owing to varying thermal or compositional buoyancy variations that are unknown to slab pulls in remote subduction zones. For example, the pulling of the subducting slabs in the western Pacific or beneath the Andes does not know the sub-ridge buoyancy and ridge axial depth variation at the southern East Pacific Rise. Nevertheless, it has been known for decades that ridge spreading rate differences do control across-ridge morphology and along-ridge topography on local and ridge segment scales, especially at slow-spreading ridges (e.g. Macdonald, 1982; Macdonald *et al.*, 1988; Sempere *et al.*, 1990; Sinton *et al.*, 1991; Grindlay *et al.*, 1991; Niu & Batiza, 1993; Niu *et al.*, 2001; Dick *et al.*, 2003). These local and segment-scale variations of ridge depth and morphology are most probably of lithospheric origin and isostatically uncompensated (i.e. dynamic topography or morphology). The effects of these features, if any, thus must be removed to reveal the origin of the correlated variations of MORB chemistry with ridge axial depth on a global scale. Klein & Langmuir (1987) and Gale *et al.* (2014) used regionally smoothed ridge axial depth to obtain an average depth value for a given ridge segment. This requires assumptions on how to smooth and how to choose a segment depth value. Instead, Niu & O'Hara (2008) made no assumptions, but used actual MORB sample depths [see below and also fig. 3 of Niu & O'Hara (2008)].

The meaning of MORB chemistry–ridge depth correlation

As above for elucidating the spreading rate effect, to effectively deconvolve the effect of processes that lead to ridge axial depth variations from the effects of all other probable or possible variables, it is desirable to average MORB chemistry with respect to ridge axial depth intervals. The averaging is not arbitrary, but follows basic principles (Niu & O'Hara, 2008), as listed here.

1. A 250 m depth interval is chosen because this depth interval size approximates the ridge depth variation over ~500 km regional scale-lengths. This gives >20 average data points with which to work. This number of data points is large enough to be statistically significant without compromising first-order systematics, but small enough to smooth out secondary effects while making the first-order global systematics prominent.
2. The averaging uses actual sample depths regardless of geographical location and ocean basin (i.e. the Pacific, Atlantic and Indian Oceans).
3. Such heavy averaging averages out the effects of (a) spreading rate variation, (b) local-scale fertile source compositional heterogeneity [including the arbitrary normal (N-) and enriched (E-)type MORB division], and (c) dynamic topography on regional and ridge segment scales (see above) to objectively observe the significance of MORB chemistry variation with respect to ridge axial depth.

Figure 7 is modified from Niu & O'Hara (2008). The 22 data points represent heavy averages of 9130 global

MORB data with MgO $\geq$ 7 wt %, corrected to Mg# = 0·72 within each of the 22 depth intervals (bins) of 250 m from actual ridge depths of ~250 to 5750 m below sea level (see Niu & O'Hara, 2008, fig. 3). Figure 7a and b shows significant correlations of MORB Ti_{72}, Al_{72}, Fe_{72}, Mg_{72}, Ca_{72}, Na_{72} and Ca_{72}/Al_{72} with ridge axial depth. Such correlations suggest a genetic relationship between MORB chemistry and ridge axial depth. However, this relationship, cannot be a 'cause and effect' one because ridge axial depth (water depth) cannot physically control MORB chemistry. I consider that the correlated variations of MORB chemistry with ridge axial depth in Fig. 7a and b are two different effects of a common cause. What is this common cause?

MORB chemistry–ridge depth correlation results from mantle compositional variation

Niu & O'Hara (2008) demonstrated explicitly that the intrinsic cause is the fertile mantle major element compositional variation. This is because fertile mantle major element compositions determine (1) variation in both composition and mode of mantle mineralogy, (2) variation of mantle density, (3) variation of ridge axial depth because of the mantle density variation, (4) source-inherited MORB compositional variation, (5) density-controlled variation in the maximum extent of mantle upwelling, (6) apparent variation in the extent of melting, and (7) the correlated variation of MORB chemistry with ridge axial depth. These physically straightforward, logically sound and geologically simple demonstrations are summarized in Fig. 7c.

The physical significance of the correlation between MORB chemistry and ridge axial depth is shown in Fig. 7 in the form of schematic illustrations, which are convenient for conceptual clarity [see Niu & O'Hara (2008) for quantitative analysis; their figs 13–19 and related discussion]. It has long been recognized that source rock compositions exert a key control on the resulting magmas, as summarized by Cox (1992): 'the most fundamental thing to understand is that the spectrum of compositions we see is controlled in the first place by the composition of the Earth itself. Just as in the simplest phase diagram the course of evolution of residual liquids by fractionation, or the course of liquid evolution during partial melting, is controlled by the starting composition, so in the Earth the range of igneous rocks is constrained by the original materials'. This simple concept of source control has been repeatedly demonstrated experimentally (see Jaques & Green, 1980; Green, 2015; Green & Falloon, 2015), and also well documented observationally (e.g. Mahoney *et al.*, 1994; Niu *et al.*, 1996, 1999, 2001, 2002*a*; Castillo *et al.*, 1998, 2000). Furthermore, on the basis of their detailed petrology and geochemistry study of several ridge segments along the northern Mid-Atlantic Ridge, Niu *et al.* (2001) recognized the dynamic role of mantle source compositional variation: 'Mantle compositional control on the extent of mantle melting, crust production, gravity anomaly, ridge morphology, and ridge segmentation'.

Indeed, as demonstrated by Niu & O'Hara (2008), the simplest interpretation is that the MORB major element compositional systematics illustrated in Fig. 7a and b largely derive from the fertile mantle compositional systematics. That is, with increasing ridge axial depth, MORB Ti_{72}, Al_{72} and Na_{72} increase whereas Fe_{72}, Mg_{72}, Ca_{72} and Ca_{72}/Al_{72} decrease, reflecting variations in the fertile mantle source composition. In other words, corresponding to the increasing ridge axial depth, the sub-ridge mantle source increases in TiO_2, Al_2O_3 and Na_2O, and decreases in FeO, MgO, CaO and CaO/Al_2O_3, becoming progressively less depleted (or more enriched) in a basaltic melt component. This correspondence becomes physically straightforward if we consider the source mineralogy as a function of the major element compositions (Niu, 1997). Correlated with increasing ridge depth, the mantle source region is progressively (1) enriched in pyroxene over olivine (or higher pyroxene/olivine ratio) because of decreasing FeO and MgO, (2) enriched in jadeite over diopside (or higher jadeite/diopside ratio) in clinopyroxene because of increasing Na_2O and Al_2O_3 and decreasing CaO and MgO, and (3) enriched in garnet because of increasing Al_2O_3. These mineralogical systematics consistently indicate increasing asthenospheric mantle density from beneath shallow ridges to beneath deep ridges (see Niu & Batiza, 1991*b*, 1991*c*; Niu *et al.*, 2003), which explains in terms of isostasy why the progressively deeper ridge is underlain by progressively more enriched (or less depleted) denser mantle and why there is such MORB chemistry–ridge depth correlation as demonstrated quantitatively by Niu & O'Hara (2008) (see their figs 13–19 and detailed discussion) with the compensation depth probably in the mantle Transition Zone (Niu & O'Hara, 2008).

This fertile mantle compositional variation controlled mantle density variation can in turn have a physical feedback on ridge dynamics. Because the sub-ridge mantle upwelling is a passive response to plate separation (McKenzie & Bickle, 1988), and because the extent of the upwelling (i.e. $P_o - P_f$ in Fig. 7c) determines the extent of decompression melting ($F \propto P_o - P_f$), the dense fertile mantle beneath deep ridges thus has restricted upwelling (isostatic control), which gives way to conductive cooling to a deep level, forces melting to stop at such a deep level, leads to a short melting interval, and thus produces less melt and probably a thin magmatic crust relative to the less dense (more refractory) fertile mantle beneath shallow ridges as illustrated in Fig. 7c (see Niu & O'Hara, 2008). This increased final depth of melting (P_f), the increased thickness of the 'cold thermal boundary layer' (CTBL), and hence the reduced extent of decompression melting ($F \propto P_o - P_f$) in response to the increased fertility and density of the MORB mantle source beneath deep ridges collectively result from a direct physical control; that is, the well-understood 'lid effect' (Niu *et al.*, 2011). The effect of this physical

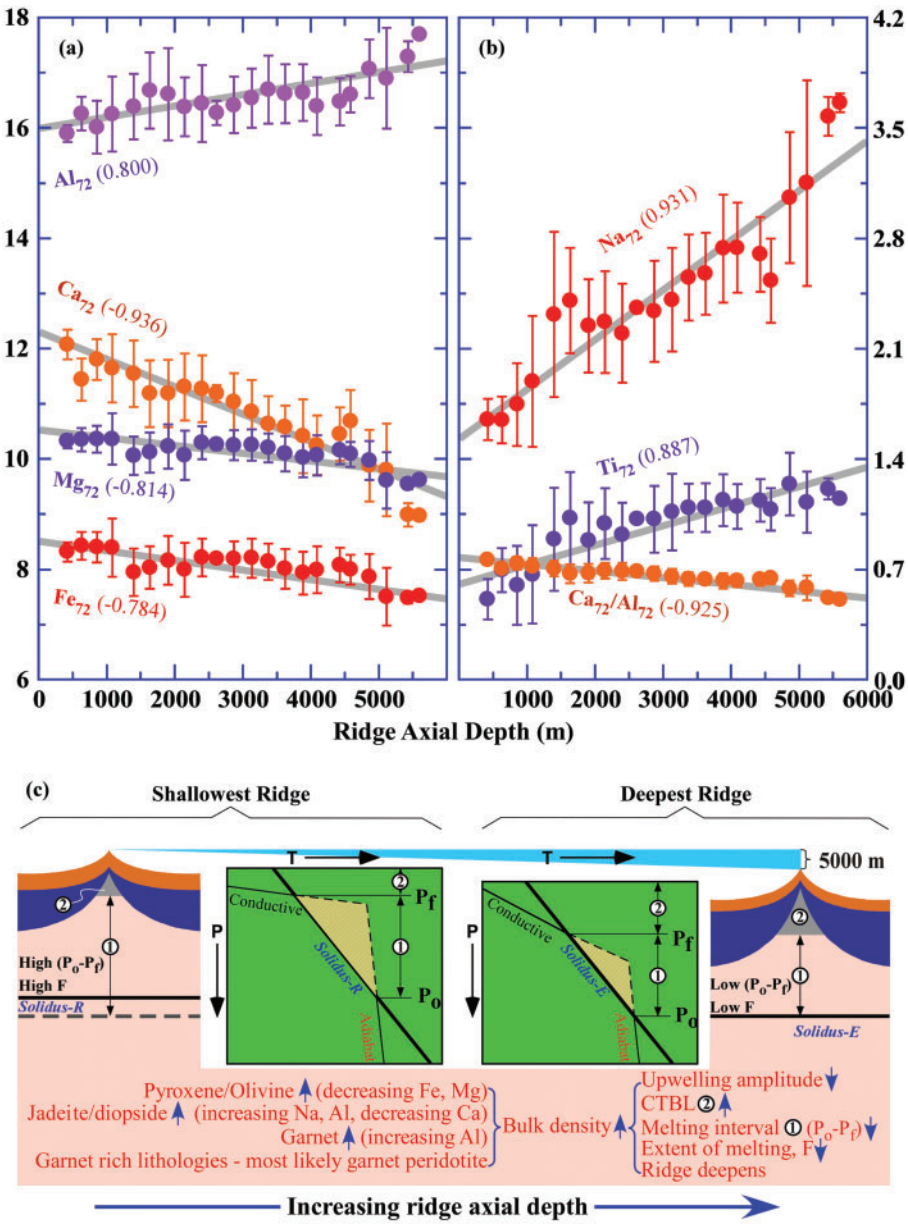

Fig. 7. (a, b) Modified from Niu & O'Hara (2008) to emphasize that, except for SiO_2, all the major element oxides (TiO_2, Al_2O_3, FeO, MgO, CaO, Na_2O and CaO/Al_2O_3), not just FeO and Na_2O, of the global MORB data after correction for the effects of cooling-dominated crustal-level processes to Mg# = 0·72, show significant intercorrelations and systematic correlations with ocean ridge axial depth. Such correlations are most consistent with fertile MORB mantle source compositional variation. The fertile mantle source is progressively more enriched (or less depleted) from beneath shallow ridges than beneath deep ridges, pointing to increasing modal garnet, jadeite/diopside ratio in clinopyroxene, and pyroxenes/olivine ratio, and thus a progressively denser mineral assemblage towards deep ridges as shown in (c). This explains straightforwardly why deep ridges are deep—fertile asthenospheric mantle is denser than more depleted mantle (see Niu *et al.*, 2003), thus resulting in deeper ridges. Shallower ridges are underlain by more depleted asthenospheric mantle and controlled by isostasy (see Niu & O'Hara, 2008, figs 13 and 14 and accompanying discussion). In addition, dense fertile mantle beneath deep ridges upwells reluctantly in response to plate separation, which leads to a limited extent of upwelling, allowing conductive cooling to penetrate to a great depth, making a thickened cold thermal boundary layer (CTBL; the gray triangular region labeled '2' in the illustration), forcing melting to stop at a deep level (P_f), resulting in a short melting interval ($P_o - P_f$) and less melting, and probably producing a thin magmatic crust relative to the more refractory fertile mantle beneath shallow ridges. The shaded triangular areas in the *P*–*T* diagrams illustrate conceptually the difference in melt production that is proportional to the height of the decompression melting intervals ($P_o - P_f$). Thus, deep ridge MORB have signatures of apparently lower extents of melting than shallow ridge MORB [see (a) and (b)] superimposed on the fertile mantle compositional inheritance [see details given by Niu & O'Hara (2008)]. An important point here is that globally the solidus depth (P_o) beneath ocean ridges away from mantle plumes (or anomalous mantle with abundant volatiles and alkalis) is essentially constant or varies little (e.g. $T_o < \sim 50$ K if any; see Niu & O'Hara, 2008). In contrast, the final depth of melting (P_f) can vary because of varying thickness of the CTBL, termed the 'lid effect', which is conspicuous for intra-plate ocean island basalts (see Niu *et al.*, 2011), but is also detectable beneath ocean ridges as the result of plate spreading rate variation as demonstrated by Niu & Hékinian (1997*a*) and further illustrated in Fig. 8 using the new global dataset of Gale *et al.* (2014).

feedback on MORB chemistry is expected to be small, but produces the same systematics as those inherited from fertile source compositions and thus amplifies the MORB chemistry correlation with ridge axial depth as in Fig. 7b and c.

Hence, the global MORB compositional systematics (Fig. 7b and c) are the net effect of (1) fertile mantle source inheritance and (2) varying extents of melting controlled by the varying extent of upwelling and decompression melting as the result of mantle density variations ultimately still controlled by fertile mantle compositional variation. Dick and co-workers have recently offered supporting case studies on the effect of fertile mantle compositional control on MORB chemistry and ridge depth (Zhou & Dick, 2013; Dick & Zhou, 2015).

The overstated mantle temperature variation is secondary or has negligible effect on the MORB chemistry–ridge depth correlation

Klein & Langmuir (1987), Langmuir *et al.* (1992) and Gale *et al.* (2014) used the large Fe_8 variation (on average ~5 Fe units; Figs 1–6) to argue for large mantle temperature variations of ~250 K beneath global ocean ridges (this refers to mantle solidus depth variation, ΔP_o, and corresponding solidus temperature variation, ΔT_o) as the cause of the MORB chemistry–ridge depth correlation. Because Fe_8 (and their $Fe_{90} = Fe_8$; Fig. 3b) is not a mantle signature, but a highly and variably evolved crustal-level signature with Mg# = 0·56–0·68 that cannot be used to infer mantle conditions in the first place, there is no petrological evidence for large mantle potential temperature variations along the global ocean ridges. Given the small thermal expansion coefficient of 3×10^{-5} K^{-1} under upper mantle conditions, the effect of mantle temperature variation on ridge axial depth variation, if any, is negligible as vigorously demonstrated by Niu & O'Hara (2008) (e.g. 1% density reduction owing to compositional depletion is equivalent to temperature increase of ~330 K). Hence, mantle temperature variation as the cause of ridge depth variation can be ruled out on the basis of simple mineral physics. To defend the interpretation of mantle temperature control, Langmuir & co-workers used ridge axial depth as a constraint for mantle temperature variation (Dalton *et al.*, 2014); their supporting argument is the low seismic velocity in the deep mantle (>300 km) beneath Iceland and adjacent shallow ridges. Evidently, using ridge depth as a mantle temperature constraint is subjective and circular, rather than justified evidence, because this argument neglects the intrinsic control of fertile mantle compositional variation on the physical properties and dynamic role of the mantle, as well as on MORB compositional variation.

In this context, it is conceptually important not to confuse plate tectonics with mantle plumes because they have no genetic connection and represent different modes of Earth's cooling. It is well understood that plate tectonics is driven by the top cold thermal boundary layer (lithospheric plates) that cools the mantle, drives major aspects of mantle convection and explains seafloor subduction and ridge dynamics (McKenzie & Bickle, 1988; Davies & Richards, 1992), whereas mantle plumes are driven by the basal hot thermal boundary layer (core–mantle boundary) (e.g. Richards *et al.*, 1989; Campbell & Griffiths, 1990; Davies & Richards, 1992) despite some debate (e.g. Davies, 2005; Foulger, 2005; Niu, 2005*b*). However, when mantle plumes rise to reach the lithospheric plates, interaction between the two can take place. Because the lithosphere is the thinnest at ridges, such interaction is best expressed as plume–ridge interactions (e.g. Ito *et al.*, 2003; Niu & Hékinian, 2004). To study ridge processes of plate tectonic origin, we should study ridges uninfluenced by hotspots or mantle plumes. Hence, to use the seismic low V_s anomaly at >300 km depth beneath Iceland (Dalton *et al.*, 2014; Gale *et al.*, 2014) that is absent elsewhere beneath global ocean ridges as evidence of a hot ridge of plate spreading origin and as evidence of large mantle temperature variations beneath global ocean ridges is inappropriate. In fact, the invoked large mantle temperature variation disappears when data from plume-influenced ridges are removed (see Niu & Hékinian, 1997*a*; Niu & O'Hara, 2008; Regelous *et al.*, 2016; also see below). There is no evidence of any kind for large mantle temperature variation beneath ridges away from mantle plumes.

I will specifically discuss in a later section why MORB melts do not preserve the solidus conditions (i.e. P_o and T_o) as previously elaborated (Niu, 1997).

The meaning of MORB chemistry–spreading rate correlation

Because ocean ridges are of plate tectonic origin, and because sub-ridge mantle upwelling is a passive response to plate separation, the rate of mantle upwelling must be positively related to plate spreading rate (e.g. Reid & Jackson, 1981; Phipps Morgan, 1987; Niu, 1997). This means that the sub-ridge mantle thermal structure and extent of decompression melting must also vary as a function of plate spreading rate. Indeed, Niu & Hékinian (1997*a*) used the then available global MORB data (Niu & Batiza, 1993) together with the available abyssal peridotite data (Dick & Fisher, 1984; Dick *et al.*, 1984; Dick, 1989; Johnson *et al.*, 1990; Niu & Hékinian, 1997*b*) to demonstrate that the extent of sub-ridge mantle melting increases with increasing spreading rate as anticipated, and as recently confirmed with an updated dataset (Regelous *et al.*, 2016). Figure 8a–c is reproduced from the spreading rate interval (bin width 20 mm a^{-1}) averaged MORB data of Niu & Hékinian (1997*a*), plotted as a function of full spreading rate. As above, heavy averaging is required to remove the effects of ridge axial depth variation and location-related mantle source heterogeneity variation on varying scales (including the arbitrary N- and E-type MORB

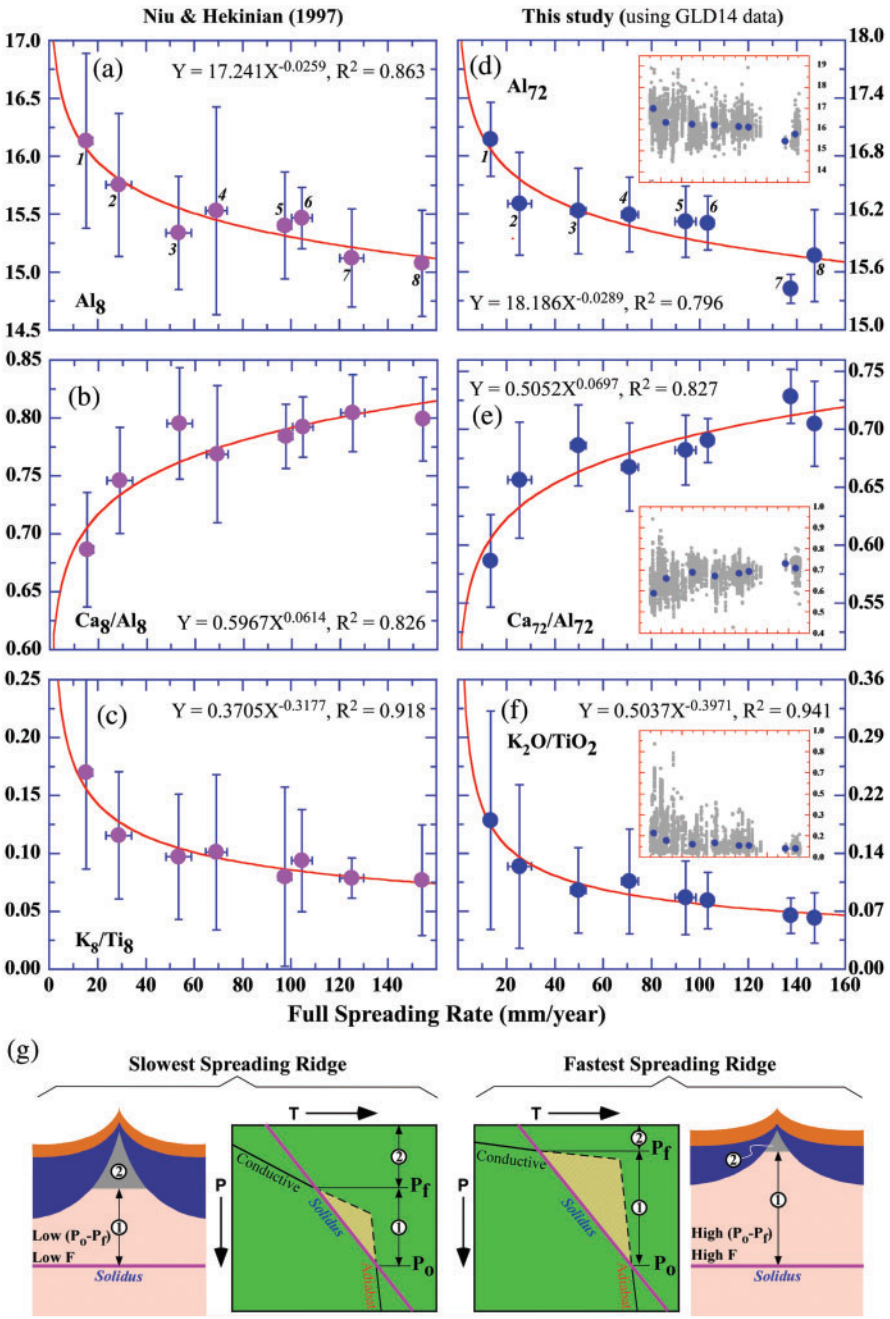

Fig. 8. Plots (a)–(c) from Niu & Hékinian [1997*a*; (c) was not shown then] together with the then available abyssal peridotite data allowed them to conclude that the extent of mantle melting beneath ocean ridges increases with increasing plate spreading rate. However, Gale *et al.* (2014) concluded (p. 1080): 'There is no correlation between the chemical parameters and spreading rate.' Plots in (d)–(f) use the new dataset of Gale *et al.* (2014) (GLD14) to show essentially the same as shown by Niu & Hékinian (1997*a*); that is, that decreasing Al_{72} (d) and Al_8 (a), increasing Ca_{72}/Al_{72} (e) and Ca_8/Al_8 (b), and decreasing K_2O/TiO_2 (f) and K_8/Ti_8 (c) with increasing spreading rate are simply and straightforwardly the result of increasing extent of melting. This spreading rate dependent extent of melting is a consequence of the spreading rate controlled lid effect as illustrated in (g), where notations are the same as in Fig. 7c. The numerals next to the data points in (a) and (d) denote '20 mm a^{-1}' spreading rate intervals for averaging. Details for (a) and (b) have been given by Niu & Hékinian (1997*a*). Details in (d)–(f) (the insets show all the data and averages) are as follows: *1*, <20 mm a^{-1}, $n = 891$ samples; *2*, 20–40 mm a^{-1}, $n = 2163$; *3*, 40–60 mm a^{-1}, $n = 1923$; *4*, 60–80 mm a^{-1}, $n = 1228$; *5*, 80–100 mm a^{-1}, $n = 1406$; *6*, 100–120 mm a^{-1}, $n = 1130$; *7*, 120–140 mm a^{-1}, $n = 7$; *8*, 120–140 mm a^{-1}, $n = 236$. The heavy averaging is necessary to examine objectively the presence and significance of any spreading rate effect by averaging out all other non-spreading rate factors (e.g. effects of fertile source variation, including the arbitrary N- and E-type MORB, ridge axial depth variation and uncertainties associated with the correction procedures). Samples with seawater depth <1500 m are excluded, as are those from plumes and plume-influenced ridges (these are samples from Iceland, near-Iceland ridges and the Red Sea) as indicated in Fig. 9a. The reason for choosing <1500 m depth is because most normal ridges have axial depths >2000 m, but there are ridges far away from plumes or hotspots that can be as shallow as ~1500 m; for example, the ridge OH-1 south of the Oceanographer Fracture Zone at ~35°N MAR (Niu *et al.*, 2001).

division) to reveal if there indeed exists any genuine correlation between MORB chemistry and plate spreading rate. As Al is an incompatible element and K is more incompatible than Ti during sub-ridge mantle melting, the decreasing Al_8 and K_8/Ti_8 and increasing Ca_8/Al_8 with increasing spreading rate are a straightforward expression of an extent of mantle melting that increases with increasing spreading rate. Figure 8g provides a straightforward illustration in terms of the lid effect (i.e. the CTBL thickness) as to why the extent of mantle melting increases with increasing spreading rate. Because the rate of mantle upwelling increases with increasing plate spreading rate (see above), fast upwelling beneath fast-spreading ridges allows the adiabat to extend to a shallower level against conductive cooling to the surface. By contrast, with slower upwelling beneath slow-spreading ridges, conductive cooling to the surface extends to a greater depth against the adiabat. Hence, the depth of P_f decreases and the decompression interval ($P_o - P_f$) increases with increasing spreading rate, hence the extent of melting F ($\propto P_o - P_f$) increases with increasing plate spreading rate.

However, Gale *et al.* (2014) refuted the demonstration and interpretation by Niu & Hékinian (1997*a*) by stating: 'There is no correlation between the chemical parameters and spreading rate' (p. 1080). Figure 8d–f is based on the Gale *et al.* (2014) data and argues against their unfounded statement, confirming the findings and demonstration by Niu & Hékinian (1997*a*) that the extent of sub-ridge mantle melting increases with increasing spreading rate. It is important to compare Fig. 8a–c with Fig. 8d–f. The conclusion based on the 20 years older MORB dataset remains valid and is seen in the newest data.

We should emphasize that the petrological and geochemical consequences of plate spreading rate variation have long been recognized, such as isotopic variability (Batiza, 1984), MORB chemical variation trends (Niu & Batiza, 1993), magma chamber processes (Sinton & Detrick, 1992), crustal-level thermal and magmatic structures (Chen, 1992; Rubin & Sinton, 2007), shallow mantle thermal structure (Reid & Jackson, 1981; Niu & Hékinian, 1997*a*), ridge morphology / topography (e.g. Macdonald, 1982; Macdonald *et al.*, 1998; Dick *et al.*, 2003) and gravity patterns (Lin & Phipps Morgan, 1992).

FURTHER INSIGHTS FROM OBSERVATIONS AND BASIC PETROLOGY

The above has illustrated that to understand the physical controls on ocean ridge processes and MORB petrogenesis, the logical approach is to isolate the effects of different physical observables. This is conceptually the same as mathematically seeking partial derivatives for a particular variable while keeping all other variables held constant (Niu & O'Hara, 2008). For example, to evaluate the effects of plate spreading rate variation on MORB petrogenesis, it is best to average petrological parameters with respect to spreading rate intervals so that the potential effects of other variables (e.g. ridge depth variation, mantle source heterogeneity on varying scales within and between ocean basins) can be largely or effectively averaged out. Likewise, to decipher the effects of processes that lead to global ridge axial depth variation on MORB petrogenesis, it is best to average petrological parameters with respect to ridge axial depth intervals so that possible effects by other variables (e.g. spreading rate variation, dynamic topography on regional and ridge segment scales as well as mantle compositional heterogeneity on all scales within and between ocean basins) can be effectively averaged out. This approach offers us new insights.

Effects of spreading rate variation on ridge axial depth and mantle melting

We have demonstrated in Fig. 8a–f that the extent of mantle melting decreases with decreasing spreading rate (see Niu & Hékinian, 1997*a*), which is a straightforward consequence of the 'lid effect' as illustrated in Fig. 8g. Because the sub-ridge mantle upwelling rate is, in an ideal situation, half of the full spreading rate (Phipps Morgan, 1987; Niu, 1997), the subdued upwelling beneath a slow-spreading ridge should lead to a deep ridge depth because conductive cooling (1) overcomes adiabatic upwelling, (2) thickens the cold (and dense) thermal boundary layer (CTBL), (3) deepens P_f, (4) reduces the $P_o - P_f$ interval, (5) lowers the extent of decompression melting, and predictably (6) produces thinner magmatic crust. This is correct in terms of basic petrology and straightforward physics. However, this anticipated correlation between ridge depth and spreading rate is not obvious in Fig. 9a. The data points are still scattered even after plume- or hotspot-influenced shallow ridges ($<$1500 m) are removed. However, as done for MORB chemistry, if we average ridge depth values with respect to the same spreading rate intervals, an expected trend emerges as indicated by the red filled circles.

Figure 9b plots only the spreading rate interval averages with 2s error bars. The topology of the power-law fitting curve is essentially the same as those of the petrological parameters in Fig. 8, with a flatter trend at spreading rates $>$50 mm a^{-1} and a rapid change at $<$40 mm a^{-1}. This is the first-time revelation of the otherwise long anticipated systematics, and points to the first-order genetic connections among spreading rate, ridge depth and petrological parameters. However, for ridges with spreading rates $>$50 mm a^{-1}, the ridge depth is essentially constant, but the petrological parameters define first-order trends that are not horizontal, and have slopes consistent with a spreading rate dependent extent of melting (Fig. 8). The average depth for ridges with spreading rates $<$40 mm a^{-1} progressively and significantly deepens with decreasing spreading rate. Because of the fact that all the average

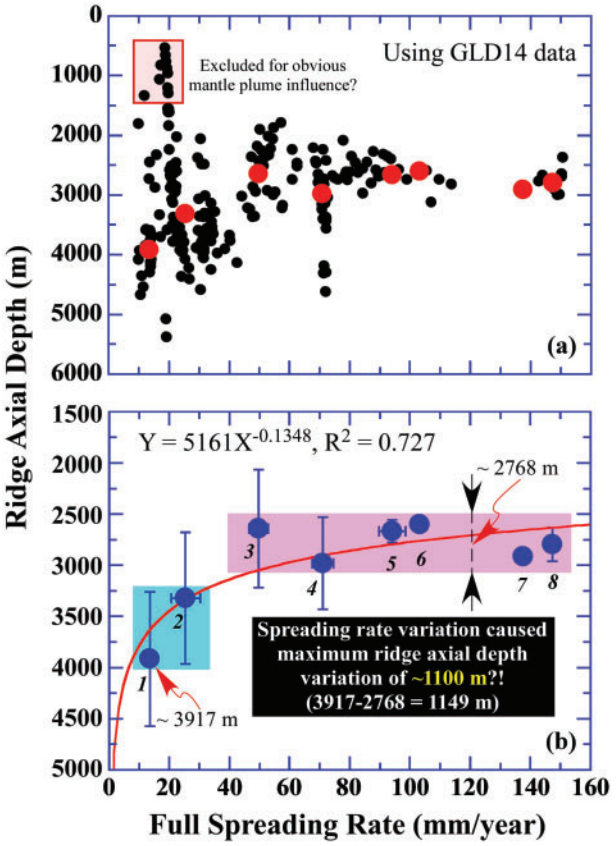

Fig. 9. (a) Plot of ridge segment depths as a function of spreading rate using the Gale *et al.* (2014) (GLD14) data, which show no simple systematics even when excluding sample sites influenced by mantle plumes or hotspots with depths <1500 m as indicated (see Fig. 8). Hence, we cannot simply state that ocean ridge depth increases with decreasing spreading rate. The red filled circles are ridge depth interval averages as described in the Fig. 8 caption. (b) As (a), but showing only the depth interval averages with 2σ error bars. The topology of the power-law fitting curve is essentially the same as those of the petrological parameters in Fig. 8 with a flatter trend at spreading rates >50 mm a^{-1} and a rapid change with further spreading rate decrease. This points to the first-order genetic connections between spreading rate, ridge depth and petrological parameters. However, for the ridges with spreading rates >50 mm a^{-1}, the ridge depths define an essentially horizontal band (~0 slope; the purple band), but the petrological parameters define first-order trends that are not horizontal, and have slopes all consistent with a spreading rate dependent extent of melting (Fig. 8). The average depths for ridges with spreading rates <40 mm a^{-1} are progressively and significantly deeper with decreasing spreading rate (light blue rectangle). Because of the fact that all the depth averages result from ridge depth interval averages with the potential effects of all other variables averaged out, the ~1100 m depth difference may be the maximum (within uncertainties) ridge depth deepening as the result of reduced spreading rate alone.

ridge depth values are spreading rate interval averages with the potential effects of all other variables being averaged out, the ~1100 m depth difference may be the maximum (with uncertainties to be verified) ridge depth deepening as the result of reduced spreading rate alone, as indicated in Fig. 9b.

A recent study by Regelous *et al.* (2016), using an updated abyssal peridotite dataset and the Gale *et al.* (2014) MORB dataset, confirmed the recognition by Niu & Hékinian (1997*a*; also Niu & O'Hara, 2014) that the extent of ridge mantle melting decreases with decreasing spreading rate, especially beneath slow-spreading ridges as demonstrated above (Fig. 8). Regelous *et al.* further concluded, however, that this rules out the effect of fertile mantle compositional variation. This latter statement is imprecise and incorrect. Let us examine why this statement needs correction. In Fig. 7 the correlations of MORB chemistry with ridge depth are best interpreted as mantle major element compositional variation as per Niu & O'Hara (2008), and provide no information on spreading rate effect because this effect is averaged out in these plots. The Fig. 8 correlations of MORB chemistry with spreading rate are consistent with spreading rate-dependent varying extent of melting (as shown by these authors), but yield no information on ridge depth effects because these are again averaged out. Hence, on the basis of Fig. 8 we cannot rule out the effect of ridge depth and mantle source effects. Now, we can see by comparing Fig. 8 and Fig. 9 that the largest MORB compositional variation occurs at slow spreading rates of <40 mm a^{-1}, which corresponds, conservatively, to a ridge axial depth variation of ~3200 m to ~4200 m. Within this depth range, we see no constant, but a significantly systematic MORB compositional variation in Fig. 7.

Therefore, it is conceptually important and correct to state that globally primitive MORB major element compositions (i.e. MORB melts with Mg# > 0·72) are largely controlled by both fertile mantle compositional variation (e.g. Fig. 7) and plate spreading rate variation (Fig. 8) with the spreading rate effect being especially prominent at very slow-spreading ridges (Figs 8 and 9).

MORB melts preserve no signature of P_o and T_o, but signature of P_f and T_f

By stating that global MORB major element compositional variations (e.g. Fe_8, Fe_{90}) result from mantle (potential) temperature variations of ~250 K (Klein & Langmuir, 1987; Langmuir *et al.*, 1992; Dalton *et al.*, 2014; Gale *et al.*, 2014), this specifically refers to variation of the depth at which upwelling mantle intersects the solidus; that is, the initial depth of melting P_o and the corresponding T_o, as schematically shown in Fig. 10. Prior to the introduction of the final depth of melting P_f and the corresponding T_f (Niu & Batiza, 1991*a*), the ridge mantle decompression melting was thought to continue up to the base of the crust (Klein & Langmuir, 1987; McKenzie & Bickle, 1988). It follows that a hotter parcel of upwelling mantle would intersect the solidus deeper, have a longer melting column and produce more melt with the signature of higher pressure (high Fe_8) and higher extent (low Na_8) of melting, whereas a cooler parcel of upwelling mantle would intersect the solidus shallower, have a shorter melting column and produce less melt with the signature of a

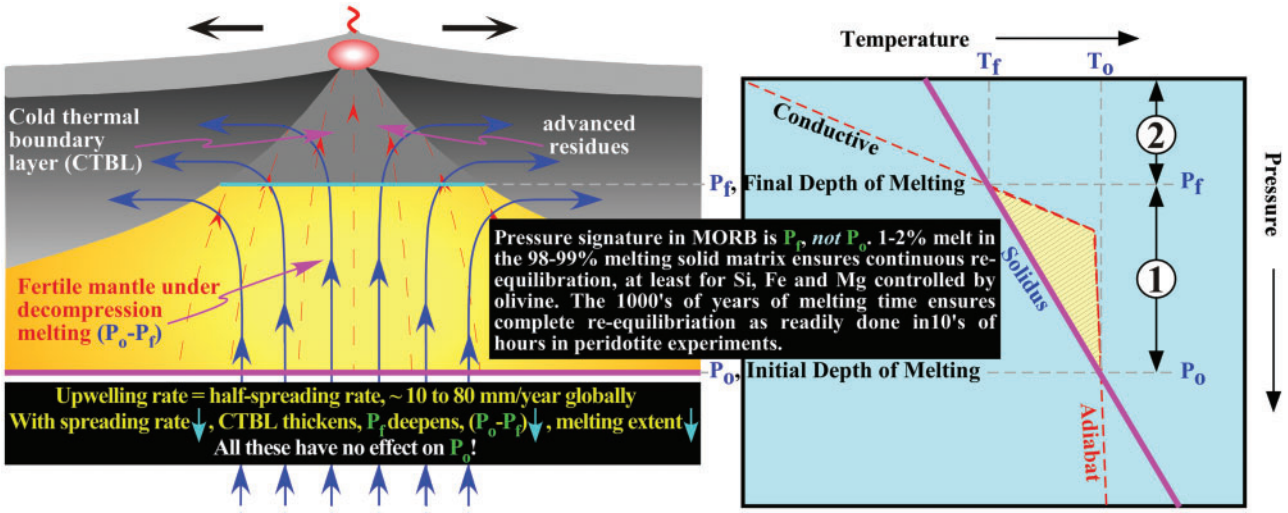

Fig. 10. Schematic illustration (left) and qualitative illustration (right) of sub-ridge thermal structure with explanation of the elements (see Figs 7 and 8). The plate separation induced decompression melting begins when the upwelling mantle intersects the solidus at P_o (at corresponding T_o) and continues until the upwelling mantle reaches P_f (at corresponding T_f), the final depth of melting or melt–solid equilibration, which is the base of the cold thermal boundary layer beneath the ridge. Because of its buoyancy, the melt (red-arrowed thin dashed lines) ascends faster than the residual solids (blue-arrowed thick lines). The melt is extracted to form the ocean crust whereas the residue contributes to the lithospheric mantle beneath the crust (shallow portions sampled as abyssal peridotites). The globally large mantle (potential) temperature variation of ~250 K claimed by Klein & Langmuir (1987) and Gale *et al.* (2014) to be preserved in MORB chemistry refers to large T_o and P_o variation. The 'lid effect' argued by Niu & O'Hara (2008) to be preserved in MORB chemistry here refers to T_f and P_f, either because of mantle density and related decompression melting (Fig. 7; Niu & O'Hara, 2008) or because of plate spreading rate variations and related decompression melting (Fig. 7; Niu & Hékinian, 1997*a*,*b*). It should be noted that because of melt–solid re-equilibration during decompression melting (P_o–P_f) on a time scale of thousands of years (re-equilibration is achieved in tens of hours experimentally), the MORB melts do not record the signature of P_o and T_o; hence there is no petrological evidence for large mantle potential temperature variation of ~250 K beneath global ocean ridges.

lower pressure (low Fe_8) and lower extent (high Na_8) of melting.

Niu and co-authors (Niu, 1997, 2004; Niu & Hékinian, 1997*a*,*b*; Niu & O'Hara, 2008) have emphasized that there is no evidence for large mantle potential temperature variation beneath global ocean ridges. The petrological parameter Fe_8 (now also Fe_{90}) as a pressure indicator collapses (see above). Dalton *et al.* (2014) used ridge axial depth variation as evidence for large mantle potential temperature variation, but this is a circular argument and has no foundation (see above and below) because fertile mantle density variations owing to compositional variations (compositional buoyancy variation) are much more effective in causing ridge axial depth variation. Niu and co-authors advocate the presence and significance of the cold thermal boundary layer (CTBL) beneath ocean ridges because this is consistent with physical analysis (Reid & Jackson, 1981) and petrological observations (Niu, 1997, 2004; Niu & Hékinian, 1997*a*,*b*; Niu *et al.*, 1997; Niu & O'Hara, 2008) as elaborated above (Figs 7 and 8). The thickness of the CTBL determines the final depth of melting or melt–solid re-equilibration, P_f, hence affecting the decompression melting interval P_o–P_f and the extent of melting. This is called the 'lid effect' (Niu *et al.*, 2011) as elaborated above as functions of fertile mantle compositional / density variation and plate spreading rate variation with correlated variations of MORB chemistry with ridge axial depth (Fig. 7) and plate spreading rate (Fig. 8).

The key message of Fig. 10 concerns the very fundamental question as to whether the erupted MORB melts can preserve the signature of P_o and T_o. The answer is simply 'No'. The melt formed by decompression (in the depth interval P_o–P_f) will ascend because of buoyancy and melt segregation caused by matrix compaction (McKenzie, 1984). This occurs as soon as the initial porosity exceeds the permeability threshold, the value of which has varied from up to 10% (e.g. Maaloe, 1982), to ~3% (McKenzie, 1984), and to several orders of magnitude less than 1% (McKenzie, 1985; Spiegelman & Elliott, 1993) to explain the observed Th–Ra excess in MORB. However ~1% porosity may be more consistent with physical analysis (Turcotte & Phipps Morgan, 1992) and petrological constraints (Johnson *et al.*, 1990). Melt migration and ascent may occur as diffuse porous flow or network-like channeling on millimeter scales (e.g. McKenzie, 1984; Turcotte & Phipps Morgan, 1992).

Therefore, recognizing that (1) porous flow is the primary means of melt transport, (2) the time scale for melt transport from the melting region to the crust is of the order of thousands of years (e.g. McKenzie, 1984, 1985; Spiegelman & McKenzie, 1987; Rubin & Macdougall, 1988, 1990), and (3) a time of no more than tens of hours is sufficient for attaining solid–melt

equilibrium in peridotite melting experiments, low-pressure melt–solid equilibration is inevitable during melt ascent (Niu, 1997). Hence, the erupted melts will not preserve the signature of the initial depth of melting (P_o, T_o), nor the signatures of any condition in the decompression interval P_o-P_f. The pressure signature the erupted MORB melts can retain would be the final depth of melting or melt–solid equilibration of P_f and T_f, which is the condition at the base of the CTBL (= 'lid'). The MORB compositional variation as a function of ridge depth variation (composition-controlled density variation; Fig. 7) and plate spreading rate variation (Fig. 8) is the manifestation of the 'lid effect'; that is, the P_f and T_f signature preserved in MORB melts (Figs 7, 8 and 10).

Because the erupted MORB melts have lost the signature of the initial depth of mantle melting (i.e. P_o and T_o) owing to the inevitable melt–solid re-equilibration, how can we use MORB chemistry to say that large mantle potential temperature variations (~250 K) exist beneath global ocean ridges? How can we logically establish primary magmas parental to MORB with MgO as high as 19 wt % (corrected to Fe_{90}; see Fig. 3d)? In Fig. 10 it is shown explicitly that the melt produced will ascend in the form of porous flow (< ~2%) through the solid peridotite matrix (> ~98%) and undergo continuous melt–solid re-equilibration. The re-equilibration is expected to be complete during decompression melting (P_o-P_f) because of the close melt–solid contact and because the thousands of years of melting and melt segregation is long enough compared with the tens of hours required to reach equilibrium in experimental charges, especially for elements such as Si, Fe and Mg controlled by olivine, which is the dominant mantle peridotite mineral. Niu (1997) presented this argument explicitly, but I ask readers to judge objectively whether MORB melts can preserve the signature of P_o and T_o in terms of Si, Fe and Mg as presumed by Klein & Langmuir (1987), Langmuir *et al.* (1992), Dalton *et al.* (2014) and Gale *et al.* (2014).

A point that should be remembered: the meaning of the correlated compositional variations of MORB and abyssal peridotites

We should note the nature of the compositional correlation between abyssal peridotites and spatially associated MORB (Dick *et al.*, 1984) and the petrological interpretations of this correlation (Dick *et al.*, 1983; Klein & Langmuir, 1987). This correlation was effectively summarized in fig. 1 of Niu *et al.* (1997), showing a scattered but statistically significant positive linear correlation between the modal clinopyroxene (vol. %) content of abyssal peridotites and the Na_8 of spatially associated MORB (18 site averages with $R^2 = 0{\cdot}74$). Niu *et al.* (1997) proposed that when sample locations approach 'hotspots' with shallowed ridge depths, both Na_8 and modal clinopyroxene decrease, which is consistent with an increasing extent of mantle melting, influenced by hotter mantle beneath hotspots. This observation is simple and powerful. The interpretation is logical also, but may not be correct. Following a detailed bulk-rock major and trace element study of global abyssal peridotites, Niu (2004, p. 2452) could not avoid the conclusion that: 'there is no clear justification that Na_8 in MORB or cpx mode in abyssal peridotites genuinely reflects the extent of mantle melting beneath mid-ocean ridges, nor that such an inferred extent of melting reflects sub-ridge mantle potential temperature variations. The complementarity could very well be inherited from the fertile mantle sources.' This was echoed by Dick *et al.* (2007), who stated: 'As the previously analyzed peridotites are from fracture zone walls 0·5 to 14 Ma. old, and the "spatially associated basalts" are largely from the modern ridge axis, this argues for a long-term stability in magma composition and therefore mantle composition as well.' Indeed, despite the compositional complementarity between MORB (melts) and abyssal peridotites (residues), it is unlikely for the ~14 Myr old abyssal peridotites to be melting residues of the present-day MORB. Mantle thermal anomalies may be long-lived, but can decay away with time. However, compositional anomalies (and buoyancy) should be long-lasting. For this, Zhou & Dick (2013) provided a good case study.

The geodynamic significance of compositional buoyancy contrast is best manifested by the largest topographic contrast on the Earth: the compositionally buoyant continental lithosphere (the crust and mantle lithosphere) and the compositionally dense oceanic lithosphere (despite the contribution of the 'coldness' of the latter) (Niu *et al.*, 2003; Niu, 2014, 2016).

SUMMARY

1. The popular petrological parameter Fe_8 devised by Klein & Langmuir (1987) and advocated by Langmuir *et al.* (1992) and Gale *et al.* (2014) in studying MORB mantle melting conditions is misleading, as demonstrated by Niu & O'Hara (2008), because Fe_8 represents variably evolved melts with Mg# = 0·56–0·68 (Figs 1–3), which is a crustal signature and cannot be in equilibrium with mantle olivine. Recent work by Gale *et al.* (2014) showed that $Fe_8 \approx Fe_{90}$ (Fig. 3b), with the purpose of advocating Fe_8 to be the same as Fe_{90}, and to reflect melts in equilibrium with mantle olivine Fo_{90}. This is not true. Because melts with Fe_8 have Mg# = 0·56–0·68, but those with Fe_{90} are meant to have Mg# ~0·72–0·73, how can $Fe_8 \approx Fe_{90}$? (Fig. 3b). The data treatment to make $Fe_{90} \rightarrow Fe_8$ was achieved by adding varying amount of olivine, but can MORB melts have MgO as high as 19 wt % (Fig. 3d)? The most primitive MORB melts with Mg# ≥ 0·72 have ~10·5 wt % MgO (data constrained). The Gale *et al.* (2014) corrected Fe_{90} (= Fe_8) values have no relevance to actual data as they are compositionally remotely different from any MORB composition

and are beyond petrologically permitted interpolation and extrapolation (Fig. 3d).

2. Global MORB major element compositional systematics in MgO or Mg# variation diagrams are not simple liquid lines of descent (LLD; Figs 4 and 5), but the net effect of cooling-dominated, crustal-level processes (e.g. fractional crystallization, magma mixing, melt–rock assimilation / reaction and other aspects of complex open-magma chamber processes). It is petrologically justified to correct MORB melts for the crustal-level effects to Mg# $\geq$ 0·72 to be in equilibrium with mantle olivine of Fo $\geq$ 90 by using a single set of correction coefficients applicable to the global MORB dataset. Global MORB FeO values corrected to Mg# = 0·72 have Fe_{72} ~7–8 wt % (i.e. ~1·0 Fe units), which is well constrained by the global MORB data as illustrated in FeO–Mg# diagrams (Figs 4 and 5). This new demonstration using the actual data as done by Niu & O'Hara (2008), argues against the incorrect statement by Gale *et al.* (2014) that the small Fe_{72} range is due to an inaccurate correction procedure. In contrast, regardless of whether the correction procedure by Gale *et al.* (2014) to Fe_8 is justified / accurate or not, the new global MORB dataset shows that Fe_8 (= FeO at MgO = 8·0 wt %) is ~7–12·5 wt % (> ~5·5 Fe units), corresponding to Mg# = 0·56–0·69 (Figs 3–5), which cannot be used to say anything petrologically meaningful about mantle processes.
3. The correlation between MORB chemistry (Ti_{72}, Al_{72}, Fe_{72}, Mg_{72}, Ca_{72}, Na_{72}, Ca_{72}/Al_{72}) and ridge axial depth (Fig. 7) indicates a genetic relationship between the two, which is not a 'cause-and-effect' one; instead, both are different effects of a common cause. The common cause is sub-ridge fertile mantle compositional variation, which, by inference, is most consistent with varying extent of prior melting and melt extraction in terms of major elements. The least depleted (or relatively enriched) MORB source is characterized by higher TiO_2, Al_2O_3 and Na_2O, and lower FeO, MgO and CaO, and thus lower CaO/Al_2O_3 than the most depleted MORB source. Such major element compositional variation determines the mantle mineralogy with greater bulk-rock density for the progressively least depleted (or relatively enriched) source, leading to progressively deeper ridges because of isostasy (Fig. 7). Melting of such compositionally varying sources imparts the source chemical signature to the erupted MORB melts (Fig. 7a and b), leading to the observed correlation of MORB chemistry with ridge axial depth (Fig. 7).
4. Mantle density is an important physical property and its variation must have a varying control on plate separation-induced upwelling. With increasing sub-ridge mantle density, as expressed by the increasing ridge axial depth, the maximum extent of passive upwelling is progressively subdued, resulting in a slightly reduced decompression melting interval and somewhat lower extent of melting. This has an enhanced (positively superimposed) effect on the signature of source composition-inherited MORB chemistry and the correlation with ridge axial depth (Fig. 7).
5. The updated global MORB dataset provided by Gale *et al.* (2014) confirms the recognition ~20 years earlier by Niu & Hékinian (1997*a*) that the extent of sub-ridge mantle melting increases with increasing plate spreading rate, which is expected in terms of the understood physics of the way in which ocean ridges work (Fig. 8), but disproves the conclusive statement by Gale *et al.* (2014): 'There is no correlation between the chemical parameters and spreading rate.'
6. Mantle temperature variation could play a role in MORB petrogenesis, but its overstated role comes from the misleading parameter Fe_8 (and Fe_{90}), from using ridge axial depth as a constraint by neglecting the intrinsic chemical and physical controls of fertile mantle compositional variation, and from treating ridge-centered mantle plumes such as the Iceland plume as being of plate tectonic origin.
7. In addition to the incorrect data treatment by Gale et al. (2014), the argument for large mantle temperature variations has an erroneous presumption; that is, MORB melts retain the signature of their initial depth of mantle melting (P_o and T_o) in terms of Fe_8 (and Fe_{90}). The decompression melting begins at P_o and continues until P_f, during which the melt phase is continuously formed (<2%) and tends to ascend because of buoyancy, while re-equilibrating with the peridotite matrix (>98%) on a time scale of thousands of years. The continued re-equilibration is inevitable because of the long enough time for close physical contact between the melt and solid, as is readily achieved experimentally in tens of hours. This is particularly true for Si, Mg and Fe controlled by olivine, the dominant phase of the peridotite matrix (Fig. 10). Therefore, MORB melts can only retain the final depth of melting or melt–solid equilibration (i.e. P_f and T_f), not T_o and T_o, as explicitly discussed previously (Niu, 1997) and demonstrated by the fact that the most primitive MORB melts with Mg# $\geq$ 0·72 have MgO $\approx$ 10·5 wt %, not higher and not as high as 19 wt % (Fig. 3d).
8. The preservation of P_f and T_f in MORB melts illustrates that the lid effect, which has a primary control on the extent of melting, final depth of melt–solid equilibration and melt compositions for intraplate ocean island magmatism (Humphreys & Niu, 2009; Niu *et al.*, 2011), also exerts a key control on MORB petrogenesis as manifested by the correlations of MORB chemistry with ridge axial depth (Fig. 7c) and with ridge spreading rate (Fig. 8g).
9. The correlations of MORB chemistry with ridge axial depth cannot be used to rule out a plate spreading rate control. Likewise, the correlations of

MORB chemistry with plate spreading rate variation cannot be used to rule out a fertile mantle compositional control. Both fertile mantle compositional variation (expressed as large ridge axial depth variations owing to composition-determined density variations) and spreading rate variation are two primary variables that control first-order ocean ridge processes in general and MORB petrogenesis in particular.

10. It has long been anticipated that ridge axial depth should increase with decreasing plate spreading rate, but the lack of correlation between the two has been puzzling. This correlation does indeed exist after removing hotspot-influenced ridges and after averaging ridge depth values within spreading rate intervals (Fig. 9). This correlation is best described by a non-linear power-law relationship that also best describes the relationship between MORB chemistry and spreading rate. All these observations are straightforward consequences of plate tectonics.
11. The meaning of the global MORB major element compositions may continue to be debated, but the conclusions offered here are the most objective and logical, and are most consistent with petrological, geochemical, geological and geophysical principles and observations.
12. To promote scientific debate, I end this paper here by sharing my philosophy: for the same data, there can be many different interpretations, but reasonable interpretations are limited and, strictly speaking, the correct interpretation must be open-minded and objective.

FUNDING

This work was supported by Chinese NSF (Grants 41630968 and 91014003), Chinese NSF–Shandong (Grant U1606401), Chinese Academy of Sciences (Innovation Grant Y42217101L), Qingdao National Laboratory for Marine Science and Technology (Grant 2015ASKJ01), and grants from regional and local authorities (Shandong Province and City of Qingdao).

ACKNOWLEDGEMENTS

I write this paper in commemoration of Mike O'Hara for his friendship, for our scientific exchanges and for the memorable times we had over the previous ~18 years before his passing through emails, phone calls, lunchtime chats and extended visits. His constructive review of my abyssal peridotite paper for this journal (Niu, 1997) began our productive research collaboration and led to my migration from the University of Queensland to Cardiff and to Durham. We published 10 papers together on topics including subduction initiation, continental crust accretion, petrogenesis of intra-plate ocean island basalts, ocean ridge basalts and lunar rocks. Our friendly discussion and scientific debates benefited me tremendously. It may surprise some, but we actually disagreed more often than agreed and he was extremely happy when he was convinced that I was correct. An anonymous journal reviewer is thanked for the very detailed and thorough constructive comments on an early version of the paper. The comments and editorial efforts by Marjorie Wilson and Alastair Lumsden have improved the paper, for which, and for their exceptional patience, I am grateful.

REFERENCES

Baker, M. B. & Stolper, E. M. (1994). Determining the composition of high-pressure mantle melts using diamond aggregates. *Geochimica et Cosmochimica Acta* **58**, 2811–2827.

Batiza, R. (1984). Inverse relationship between Sr isotope diversity and rate of oceanic volcanism has implications for mantle heterogeneity. *Nature* **309**, 440–441.

Batiza, R. & Niu, Y. L. (1992). Petrology and magma chamber processes at the East Pacific Rise ~9°30′N. *Journal of Geophysical Research* **97**, 6779–6797.

Bryan, W. B. & Moore, J. G. (1977). Compositional variations of young basalts in mid-Atlantic ridge rift valley near Lat 36°49′N. *Geological Society of America Bulletin* **88**, 556–570.

Campbell, I. H. & Griffiths, R. W. (1990). Implications of mantle plume structure for the evolution of flood basalts. *Earth and Planetary Science Letters* **99**, 79–93.

Castillo, P. R., Natland, J. H., Niu, Y. & Lonsdale, P. (1998). Sr, Nd, and Pb isotopic variation along the Pacific ridges from 53 to 56°S: Implications for mantle and crustal dynamic processes. *Earth and Planetary Science Letters* **154**, 109–125.

Castillo, P. R., Klein, E., Bender, J., Langmuir, C., Shirey, S., Batiza, R. & White, W. (2000). Petrology and Sr, Nd, and Pb isotope geochemistry of mid-ocean ridge basalts from 11°45′N to 15°N segments of the East Pacific Rise. *Geochemistry, Geophysics, Geosystems* **1**, 1999GC000024.

Chen, Y. J. (1992). Oceanic crust thickness versus spreading rate. *Geophysical Research Letters* **19**, 753–756.

Christie, D. M. & Sinton, J. M. (1986). Major element constraints on melting, differentiation and mixing of magmas from the Galapagos 95·5°W propagating rift system. *Contributions to Mineralogy and Petrology* **94**, 274–288.

Coogan, L. A. & O'Hara, M. J. (2015). MORB differentiation: *In situ* crystallization in replenished–tapped magma chambers. *Geochimica et Cosmochimica Acta* **158**, 147–161.

Cox, K. G. (1992). The interpretation of magmatic evolution. In: Brown, G. C., Hawkesworth, C. J. & Wilson, R. C. L. (eds) *Understanding the Earth: A New Synthesis*. Cambridge University Press, pp. 115–131.

Dalton, C. A., Langmuir, C. H. & Gale, A. (2014). Geophysical and geochemical evidence for deep temperature variations beneath mid-ocean ridges. *Science* **344**, 80–83.

Danyushevsky, L. V. (1998). The effect of small amount of H_2O on fractionation of mid-ocean ridge magmas. *EOS Transactions American Geophysical Union* **79**, 375.

Davies, G. F. (2005). A case for mantle plumes. *Chinese Science Bulletin* **50**, 1541–1554.

Davies, G. F. & Richards, M. A. (1992). Mantle convection. *Journal of Geology* **100**, 151–206.

DeMets, C., Gordon, R. G., Argus, D. F. & Stein, S. (1990). Current plate motions. *Geophysical Journal International* **101**, 425–478.

Dick, H. J. B. (1989). Abyssal peridotites, very slow spreading ridges and ocean ridge magmatism. In: Saunders, A. D. & Norry, M. J. (eds) *Magmatism in the Ocean Basins.*

Geological Society, London, Special Publications **42**, 71–105.

Dick, H. J. B. & Fisher, R. L. (1984). Mineralogic studies of the residues of mantle melting: Abyssal and alpine-type peridotites. In: Kornprobst, J. (ed.) *Kimberlites II: The Mantle and Crust–Mantle Relationships. Proceedings of the Third International Kimberlite Conference*, Vol. 2. Elsevier, pp. 295–308.

Dick, H. J. B. & Zhou, H. (2015). Ocean rises are products of variable mantle composition, temperature and focused melting. *Nature Geoscience* **8**, 68–74.

Dick, H. J. B., Fisher, R. L. & Bryan, W. B. (1984). Mineralogical variability of the uppermost mantle along mid-ocean ridges. *Earth and Planetary Science Letters* **69**, 88–106.

Dick, H. J. B., Lin, J. & Schouten, H. (2003). An ultraslow-spreading class of ocean ridge. *Nature* **426**, 405–412.

Dick, H. J. B., Warren, J. M. & Shimizu, N. (2007). Global variations in abyssal peridotite composition II: what determines the major element MORB composition. American Geophysical Union Fall Meeting, Abstract #U21B-0417.

Forsyth, D. & Uyeda, S. (1975). On the relative importance of the driving forces of plate motion. *Geophysical Journal International* **43**, 163–200.

Foulger, G. R. (2005). Mantle plumes: Why the current skepticism. *Chinese Science Bulletin* **50**, 1555–1560.

Frey, F. A., Bryan, W. B. & Thompson, G. (1974). Atlantic Ocean floor: Geochemistry and petrology of basalts from Legs 2 and 3 of the Deep-Sea Drilling Project. *Journal of Geophysical Research* **79**, 5570–5527.

Gale, A., Langmuir, C. H. & Dalton, C. A. (2014). The global systematics of ocean ridge basalts and their origin. *Journal of Petrology* **55**, 1051–1082.

Green, D. H. (2015). Experimental petrology of peridotites, including effects of water and carbon on melting in the Earth's upper mantle. *Physics and Chemistry of Minerals* **42**, 95–102.

Green, D. H. & Falloon, T. J. (1998). Pyrolite: A Ringwood concept and its current expression. In: Jackson, I. (ed.) *The Earth's Mantle, Composition, Structure, and Evolution*. Cambridge University Press, pp. 311–380.

Green, D. H. & Falloon, T. J. (2005). Primary magmas at mid-ocean ridges, 'hotspots,' and other intraplate settings: Constraints on mantle potential temperature. In: Foulger, G. R., Natland, J. H., Presnall, D. C. & Anderson, D. L. (eds) *Plates, Plumes, and Paradigms. Geological Society of America, Special Papers* **388**, 217–248.

Green, D. H. & Falloon, T. J. (2015). Mantle-derived magmas: Intraplate, hot-spots and mid-ocean ridges. *Science Bulletin* **60**, 1873–1900.

Grindlay, N. R., Fox, P. J. & Macdonald, K. C. (1991). Second-order ridge axis discontinuities in the South Atlantic: Morphology, structure, and evolution. *Marine Geophysical Researches* **13**, 21–49.

Grove, T. L., Kinzler, R. J. & Bryan, W. B. (1992). Fractionation of mid-ocean ridge basalt (MORB). In: Phipps Morgan, J., Blackman, D. K. & Sinton, J. M. (eds) *Mantle Flow and Melt Generation at Mid-ocean Ridges. American Geophysical Union, Geophysical Monograph* **71**, 281–310.

Humphreys, E. R. & Niu, Y. L. (2009). On the composition of ocean island basalts (OIB): The effects of lithospheric thickness variation and mantle metasomatism. *Lithos* **112**, 118–136.

Ito, G., Lin, J. & Graham, D. (2003). Observational and theoretical studies of the dynamics of plume–mid-ocean ridge interaction. *Reviews of Geophysics* **41**, 3.1–3.24.

Jaques, A. L. & Green, D. H. (1980). Anhydrous melting of peridotite at 0–15 kb pressure and the genesis of tholeiitic basalts. *Contributions to Mineralogy and Petrology* **73**, 287–310.

Johnson, K. T. M., Dick, H. J. B. & Shimizu, N. (1990). Melting in the oceanic upper mantle: an ion microprobe study of diopsides in abyssal peridotites. *Journal of Geophysical Research* **95**, 2661–2678.

Klein, E. M. & Langmuir, C. H. (1987). Global correlations of ocean ridge basalt chemistry with axial depth and crustal thickness. *Journal of Geophysical Research* **92**, 8089–8115.

Langmuir, C. H. (1989). Geochemical consequences of *in situ* crystallization. *Nature* **340**, 199–205.

Langmuir, C. H. & Hanson, G. N. (1980). An evaluation of major element heterogeneity in the mantle sources of basalts. *Philosophical Transactions of the Royal Society of London, Series A* **297**, 383–404.

Langmuir, C. H., Bender, J. F. & Batiza, R. (1986). Petrological and tectonic segmentation of the East Pacific Rise, 5°30′–14°30′N. *Nature* **322**, 422–429.

Langmuir, C. H., Klein, E. M. & Plank, T. (1992). Petrological systematics of mid-ocean ridge basalts: Constraints on melt generation beneath ocean ridges. In: Phipps Morgan, J., Blackman, D. K. & Sinton, J. M. (eds) *Mantle Flow and Melt Generation at Mid-ocean Ridges. American Geophysical Union, Geophysical Monograph* **71**, 183–280.

Lecroart, P., Albarède, F. & Cazenave, A. (1997). Correlations of mid-ocean ridge basalt chemistry with the geoid. *Earth and Planetary Science Letters* **153**, 37–55.

Lin, J. & Phipps Morgan, J. (1992). The spreading-rate dependence of three-dimensional mid-ocean ridge gravity structure. *Geophysical Research Letters* **19**, 13–16.

Maaloe, S. (1982). Geochemical aspects of permeability controlled partial melting and fractional crystallization. *Geochimica et Cosmochimica Acta* **46**, 43–57.

Macdonald, K. C. (1982). Mid-ocean ridges: fine scale tectonic, volcanic and hydrothermal processes within the plate boundary zone. *Annual Review of Earth and Planetary Sciences* **10**, 155–190.

Macdonald, K. C., Fox, P. J., Perram, L. J., Eisen, M. F., Haymon, R. M., Miller, S. P., Carbotte, S. M., Cormier, M.-H. & Shor, A. N. (1988). A new view of the mid-ocean ridge from the behavior of ridge-axis discontinuity. *Nature* **335**, 217–225.

Mahoney, J. J., Sinton, J. M., Kurz, D. M., Macdougall, J. D., Spencer, K. J. & Lugmair, G. W. (1994). Isotope and trace element characteristics of a superfast spreading ridge: East Pacific Rise, 13–23°S. *Earth and Planetary Science Letters* **121**, 173–193.

Matzen, A. K., Baker, M. B., Beckett, J. R. & Stolper, E. M. (2011). Fe–Mg partitioning between olivine and high-magnesian melts and the nature of Hawaiian parental liquids. *Journal of Petrology* **52**, 1243–1263.

McKenzie, D. (1984). The generation and compaction of partially molten rock. *Journal of Petrology* **25**, 713–765.

McKenzie, D. (1985). ^{230}Th–^{238}U disequilirium and the melting processes beneath ridge axes. *Earth and Planetary Science Letters* **72**, 81–91.

McKenzie, D. & Bickle, M. J. (1988). The volume and composition of melt generated by extension of the lithosphere. *Journal of Petrology* **29**, 625–679.

Natland, J. H. (1989). Partial melting of a lithologically heterogeneous mantle: Inferences from crystallisation histories of magnesian abyssal tholeiites from the Siqueiros Fracture Zone. In: Saunders, A. D. & Norry, M. J. (eds) *Magmatism in the Ocean Basins. Geological Society, London, Special Publications* **42**, 41–70.

Niu, Y. L. (1997). Mantle melting and melt extraction processes beneath ocean ridges: Evidence from abyssal peridotites. *Journal of Petrology* **38**, 1047–1074.

Niu, Y. L. (2004). Bulk-rock major and trace element compositions of abyssal peridotites: Implications for mantle melting, melt extraction and post-melting processes beneath ocean ridges. *Journal of Petrology* **45**, 2423–2458.

Niu, Y. L. (2005a). Generation and evolution of basaltic magmas: Some basic concepts and a hypothesis for the origin of the Mesozoic–Cenozoic volcanism in eastern China. *Geological Journal of China Universities* **11**, 9–46.

Niu, Y. L. (2005b). On the mantle plume debate. *Chinese Science Bulletin* **50**, 1537–1540.

Niu, Y. L. (2014). Geological understanding of plate tectonics: Basic concepts, illustrations, examples and new perspectives. *Global Tectonics and Metallogeny* **10**, 23–46.

Niu, Y. L. (2016). Testing the geologically testable hypothesis on subduction initiation. *Science Bulletin* **61**, 1231–1235.

Niu, Y. L. & Batiza, R. (1991a). An empirical method for calculating melt compositions produced beneath mid-ocean ridges: application for axis and off-axis (seamounts) melting. *Journal of Geophysical Research* **96**, 21753–21777.

Niu, Y. L. & Batiza, R. (1991b). *In-situ* densities of silicate melts and minerals as a function of temperature, pressure, and composition. *Journal of Geology* **99**, 767–775.

Niu, Y. L. & Batiza, R. (1991c). DENSCAL: A program for calculating the densities of silicate melts and minerals as a function of temperature, pressure, and composition in magma generation environment. *Computers and Geosciences* **17**, 679–687.

Niu, Y. L. & Batiza, R. (1993). Chemical variation trends at fast and slow spreading ridges. *Journal of Geophysical Research* **98**, 7887–7902.

Niu, Y. L. & Batiza, R. (1994). Magmatic processes at the Mid-Atlantic Ridge ~26°S. *Journal of Geophysical Research* **99**, 19719–19740.

Niu, Y. L. & Batiza, R. (1997). Trace element evidence from seamounts for recycled oceanic crust in the eastern Pacific mantle. *Earth and Planetary Science Letters* **148**, 471–483.

Niu, Y. L. & Hékinian, R. (1997a). Spreading rate dependence of the extent of mantle melting beneath ocean ridges. *Nature* **385**, 326–329.

Niu, Y. L. & Hékinian, R. (1997b). Basaltic liquids and harzburgitic residues in the Garrett transform: A case study at fast-spreading ridges. *Earth and Planetary Science Letters* **146**, 243–258.

Niu, Y. L. & Hékinian, R. (2004). Ridge suction drives plume–ridge interactions. In: Hékinian, R., Stoffers, P. & Cheminée, J.-L. (eds) *Oceanic Hotspots*. Springer, pp. 285–307.

Niu, Y. L. & O'Hara, M. J. (2008). Global correlations of ocean ridge basalt chemistry with axial depth: A new perspective. *Journal of Petrology* **49**, 633–664.

Niu, Y. L. & O'Hara, M. J. (2009). MORB mantle hosts the missing Eu (Sr, Nb, Ta and Ti) in the continental crust: New perspectives on crustal growth, crust–mantle differentiation and chemical structure of oceanic upper mantle. *Lithos* **112**, 1–17.

Niu, Y. L. & O'Hara, M. J. (2014). A logical approach towards genuine understanding of the working of global ocean ridges, Goldschmidt Conference Abstract, 1820.

Niu, Y. L., Waggoner, D. G., Sinton, J. M. & Mahoney, J. J. (1996). Mantle source heterogeneity and melting processes beneath seafloor spreading centers: The East Pacific Rise, 18°–19°S. *Journal of Geophysical Research* **101**, 27711–27733.

Niu, Y. L., Langmuir, C. H. & Kinzler, R. J. (1997). The origin of abyssal peridotites: A new perspective. *Earth and Planetary Science Letters* **152**, 251–265.

Niu, Y. L., Collerson, K. D., Batiza, R., Wendt, J. I. & Regelous, M. (1999). The origin of E-type MORB at ridges far from mantle plumes: The East Pacific Rise at 11°20′N. *Journal of Geophysical Research* **104**, 7067–7087.

Niu, Y. L., Bideau, D., Hékinian, R. & Batiza, R. (2001). Mantle compositional control on the extent of melting, crust production, gravity anomaly and ridge morphology: a case study at the Mid-Atlantic Ridge 33–35°N. *Earth and Planetary Science Letters* **186**, 383–399.

Niu, Y. L., Regelous, M., Wendt, J. I., Batiza, R. & O'Hara, M. J. (2002a). Geochemistry of near-EPR seamounts: Importance of source vs. process and the origin of enriched mantle component. *Earth and Planetary Science Letters* **199**, 329–348.

Niu, Y. L., Gilmore, T., Mackie, S., Greig, A. & Bach, W. (2002b). Mineral chemistry, whole rock compositions, and petrogenesis of Leg 176 gabbros: Data and discussion. In: Natland, J. H., Dick, H. J. B., Miller, D. J. & Von Herzen, R. P. (Eds) *Proceedings of the Ocean Drilling Program, Scientific Results 176*. Ocean Drilling Program, pp. 1–60.

Niu, Y. L., O'Hara, M. J. & Pearce, J. A. (2003). Initiation of subduction zones as a consequence of lateral compositional buoyancy contrast within the lithosphere: A petrologic perspective. *Journal of Petrology* **44**, 851–866.

Niu, Y. L., Wilson, M., Humphreys, E. R. & O'Hara, M. J. (2011). The origin of intra-plate ocean island basalts (OIB): The lid effect and its geodynamic implications. *Journal of Petrology* **52**, 1443–1468.

O'Hara, M. J. (1968a). Are ocean floor basalts primary magmas?. *Nature* **220**, 683–686.

O'Hara, M. J. (1968b). The bearing of phase equilibria studies in synthetic and natural systems on the observation of volcanic products. *Physics of the Earth and Planetary Interiors* **3**, 236–245.

O'Hara, M. J. (1977). Geochemical evolution during fractional crystallization of a periodically refilled magma chamber. *Nature* **266**, 503–507.

O'Neill, H. St. C. & Jenner, F. E. (2012). The global pattern of trace-element distributions in ocean floor basalts. *Nature* **491**, 698–704.

Perfit, M. R. & Fornari, D. J. (1983). Geochemical studies of abyssal lavas recovered by DSRV *Alvin* from Eastern Galapagos Rift, Inca Transform, and Ecuador Rift 3. Trace element abundances and petrogenesis. *Journal of Geophysical Research* **88**, 10551–10572.

Phipps Morgan, J. (1987). Melt migration beneath mid-ocean ridge spreading centers. *Geophysical Research Letters* **14**, 1238–1241.

Regelous, M., Weinzierl, C. G. & Haase, K. M. (2016). Controls on melting at spreading ridges from correlated abyssal peridotite–mid-ocean ridge basalt composition. *Earth and Planetary Science Letters* **449**, 1–11.

Reid, I. & Jackson, H. R. (1981). Oceanic spreading rate and crustal thickness. *Marine Geophysical Researches* **5**, 165–172.

Richards, M. A., Duncan, R. A. & Courtillot, V. E. (1989). Flood basalts and hot-spot tracks: plume heads and tails. *Science* **246**, 103–107.

Roeder, P. L. & Emslie, R. F. (1970). Olivine–liquid equilibrium. *Contributions to Mineralogy and Petrology* **29**, 275–289.

Rubin, K. H. & Macdougall, J. D. (1988). ^{226}Ra excesses in mid-ocean ridge basalts and mantle melting. *Nature* **335**, 158–161.

Rubin, K. H. & Macdougall, J. D. (1990). Dating of neovolcanic MORB using (^{226}Ra/^{230}Th) disequilibrium. *Earth and Planetary Science Letters* **101**, 313–322.

Rubin, K. H. & Sinton, J. M. (2007). Inferences on mid-ocean ridge thermal and magmatic structure from MORB compositions. *Earth and Planetary Science Letters* **260**, 257–276.

Rubin, K. H., Sinton, J. M., Maclennan, J. & Hellebrand, E. (2009). Magmatic filtering of mantle compositions at mid-ocean ridge volcanoes. *Nature Geoscience* **2**, 321–328.

Schilling, J.-G., Zajac, M., Evans, R., Jonson, T., White, W., Devine, J. D. & Kingsley, T. (1983). Petrological and geochemical variations along the mid-Atlantic Ridge from 29°N to 73°N. *American Journal of Science* **283**, 510–586.

Sempere, J.-C., Purdy, G. M. & Schouten, H. (1990). Segmentation of the Mid-Atlantic Ridge between 24°N and 34°40′N. *Nature* **344**, 427–431.

Shen, Y. & Forsyth, D. W. (1995). Geochemical constraints on initial and final depths of melting beneath mid-ocean ridges. *Journal of Geophysical Research* **100**, 2211–2237.

Sinton, J. M. & Detrick, R. S. (1992). Mid-ocean ridge magma chambers. *Journal of Geophysical Research* **97**, 197–216.

Sinton, J. M., Smaglik, S. M, Mahoney, J. J. & Macdonald, K. C. (1991). Magmatic processes at superfast spreading mid-ocean ridges: glass compositional variations along the East Pacific Rise 13°–23°S. *Journal of Geophysical Research* **96**, 6133–6155.

Sobolev, A. V., Hofmann, A. W., Kuzmin, D. V., et al. (2007). The amount of recycled crust in sources of mantle-derived melts. *Science* **316**, 412–417.

Spiegelman, M. & Elliott, T. (1993). Consequences of melt transport for U-series disequilibrium in young lavas. *Earth and Planetary Science Letters* **118**, 1–20.

Spiegelman, M. & McKenzie, D. (1987). Simple 2-D models for melt extraction at mid-ocean ridges and island arcs. *Earth and Planetary Science Letters* **83**, 137–152.

Stolper, E. M. (1980). Phase diagram for mid-ocean ridge basalts: Preliminary results and implications for petrogenesis. *Contributions to Mineralogy and Petrology* **74**, 13–27.

Stone, S. & Niu, Y. L. (2009). Origin of compositional trends in clinopyroxene of oceanic gabbros and gabbroic rocks: A case study using data from ODP Hole 735B. *Journal of Volcanology and Geothermal Research* **184**, 313–322.

Sun, S.-s, Tatsumoto, M. & Schilling, J.-G. (1975). Mantle plume mixing along the Reykjanes ridge: Lead isotope evidence. *Science* **190**, 143–147.

Sun, S.-s, Nesbitt, R. W. & Sharaskin, A. Y. (1979). Geochemical characteristics of mid-ocean ridge basalts. *Earth and Planetary Science Letters* **44**, 119–138.

Turcotte, D. L. & Phipps Morgan, J. (1992). Magma migration and mantle flow beneath a mid-ocean ridge. In: Phipps Morgan, J., Blackman, D. K. & Sinton, J. M. (eds) *Mantle Flow and Melt Generation at Mid-ocean Ridges. American Geophysical Union, Geophysical Monograph* **71**, 155–182.

Walker, D., Shibata, T. & DeLong, S. E. (1979). Abyssal tholeiites from the Oceanographer Fracture Zone, II, Phase equilibria and mixing. *Contributions to Mineralogy and Petrology* **70**, 111–125.

Weaver, J. S. & Langmuir, C. H. (1990). Calculation of phase equilibrium in mineral melt systems. *Computers and Geosciences* **16**, 1–19.

Yang, Z. F. & Zhou, J. H. (2013). Can we identify source lithology of basalt? *Scientific Reports* **3**, 1–7.

Zhou, H. & Dick, H. J. B. (2013). Thin crust as evidence for depleted mantle supporting the Marion Rise. *Nature* **494**, 195–200.

Zindler, A., Staudigel, H. & Batiza, R. (1984). Isotope and trace element geochemistry of young Pacific seamounts: Implications for the scale of upper mantle heterogeneity. *Earth and Planetary Science Letters* **70**, 175–195.